DOI: 10.1002/chem.200500464

Rh-Catalyzed Asymmetric Hydrogenation of Prochiral Olefins with a Dynamic Library of Chiral TROPOS Phosphorus Ligands

Chiara Monti,[a] Cesare Gennari,*[a] Umberto Piarulli,*[b] Johannes G. de Vries,[c] André H. M. de Vries,[c] and Laurent Lefort[c]

Abstract: A library of 19 chiral tropos phosphorus ligands, based on a flexible (tropos) biphenol unit and a chiral P-bound alcohol (11 phosphites) or secondary amine (8 phosphoramidites), was synthesized. These ligands were screened, individually and as a combination of two, in the rhodium-catalyzed asymmetric hydrogenation of dehydro-α-amino acids, dehydro-β-amino acids, enamides and dimethyl itaconate. *ee* values up to 98% were obtained for the dehydro-α-amino acids, by using the best combination of ligands, a phosphite [**4**-$P(O)_2O$] and a phosphoramidite [**13**-$P(O)_2N$]. Kinetic studies of the reactions with the single ligands and with the combination of phosphite [**4**-$P(O)_2O$] and phosphoramidite [**13**-$P(O)_2N$] have shown that the phosphite, despite being less enantioselective, promotes the hydrogenation of methyl 2-acetamidoacrylate and methyl 2-acetamidocinnamate faster than the mixture of the same phosphite with the phosphoramidite, while the phosphoramidite alone is much less active. In this way, the reaction was optimized by lowering the phosphite/phosphoramidite ratio (the best ratio is 0.25 equiv phosphite/1.75 equiv phosphoramidite) with a resulting improvement of the product enantiomeric excess. A simple mathematical model for a better understanding of the variation of the enantiomeric excess with the phosphite/phosphoramidite ratio is also presented.

Keywords: amino acids · asymmetric catalysis · hydrogenation · P ligands · rhodium

Introduction

The rhodium-catalyzed asymmetric hydrogenation of prochiral olefins is a well established methodology for the industrial preparation of chiral building blocks and enantiomerically enriched amino acids.[1] Chiral bisphosphorus ligands have played a major role in this reaction since the pioneering work of Knowles and Kagan.[2] Recently, monodentate phosphorus ligands have been applied successfully, providing high enantioselectivities, sometimes even higher than the bidentate ligands.[3] In particular, readily accessible, inexpensive and highly diverse chiral monodentate ligands such as phosphoramidites, phosphites and phosphonites have been introduced,[4] which comprise different units attached to the phosphorus atom: a diol with a stereogenic axis (often binaphthol) and a N- or O- or C-substituent, which may contain additional stereogenic elements (stereocenters). In the presence of stereocenters, it is the diol stereogenic axis which usually dictates the absolute configuration of the reaction product.[4f] An important breakthrough in this area was recently made independently by Reetz and co-workers[5] and Feringa and co-workers[6] who used of a mixture of chiral monodentate P-ligands.[7] By mixing two ligands (L^a and L^b) in the presence of Rh, three species can be formed in various ratios:[8] RhL^aL^a, RhL^bL^b and RhL^aL^b. The heterocombinations allowed for better yields and enantioselectivities compared to the corresponding homocombinations.[5,6]

[a] Dr. C. Monti, Prof. Dr. C. Gennari
Dipartimento di Chimica Organica e Industriale
Centro di Eccellenza C.I.S.I.
Università degli Studi di Milano
Istituto di Scienze e Tecnologie Molecolari (ISTM) del CNR
Via G. Venezian 21, 20133 Milano (Italy)
Fax: (+39) 02-5031-4072
E-mail: cesare.gennari@unimi.it

[b] Prof. Dr. U. Piarulli
Dipartimento di Scienze Chimiche e Ambientali
Università degli Studi dell'Insubria
Via Valleggio 11, 22100 Como (Italy)
Fax: (+39) 031-238-6449
E-mail: umberto.piarulli@uninsubria.it

[c] Prof. Dr. J. G. de Vries, Dr. A. H. M. de Vries, Dr. L. Lefort
DSM Pharma Chemicals - Advanced Synthesis
Catalysis and Development, P.O. Box 18
6160 MD Geleen (The Netherlands)

Supporting information for this article is available on the WWW under http://www.chemeurj.org/ or from the author.

Usually mixtures of two chiral monodentate P-ligands (binaphthol based) were used, but also mixtures of a chiral and an achiral P-ligand were recently tested with some success.[5c,f,6b] Application of this approach to the asymmetric hydrogenation of cinnamates has recently led to an industrial process.[9,10]

Following our longstanding interest in the search for combinatorial/high-throughput approaches to enantioselective catalysis,[11] we became interested in the development of chiral phosphorus ligands for asymmetric hydrogenation comprising different elements attached to the phosphorus atom: a cheap and flexible (tropos)[12] biphenol unit and an alcohol or secondary amine, which contains stereocenters (Scheme 1).[13] This motif had recently been described by

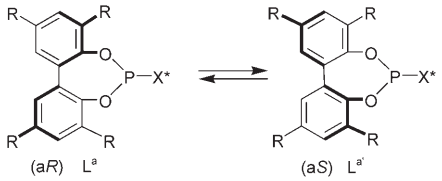

Scheme 1. Chiral phosphorus ligands based on a flexible (tropos) biphenol unit. R = H, *t*Bu, Me; X* = secondary amine or alcohol, containing stereocenters.

Alexakis and co-workers (phosphoramidite ligands) and Dieguez and co-workers (diphosphite ligands) in the enantioselective copper-catalyzed conjugate addition of diethylzinc to enones[14,15] and Me_3Al to nitroalkenes,[16] by Reetz and co-workers in the Rh-catalyzed hydrogenation (diphosphite ligands),[17] by van Leeuwen and co-workers in the Rh-catalyzed hydroformylation reaction (diphosphite ligands),[18] by Alexakis and co-workers in the enantioselective copper-catalyzed allylic substitution (phosphoramidite ligands),[19] and by Pamies, Dieguez and co-workers in the Pd-catalyzed asymmetric allylic substitution (phosphite-oxazoline and diphosphite ligands).[20] Kondo and Aoyama applied the same concept to the asymmetric Grignard cross-coupling reaction, using a phosphorus ligand based on a chiral amine with a conformationally flexible (tropos) N–Ar axis.[21]

Our ligands (Scheme 1) exist, in principle, as a mixture of two rapidly interconverting diastereomers, L^a and $L^{a'}$, differing in the conformation of the biphenol unit. Upon complexation with Rh, the ligand (L^a in equilibrium with $L^{a'}$) should give rise to three different species, namely RhL^aL^a, $RhL^aL^{a'}$, $RhL^{a'}L^{a'}$. These three diastereomeric species, which might be interconverting, are generated in proportions which most likely differ from the statistical value (1:2:1). The novelty of our approach consists in the use of a combination of two of these ligands (L^a in equilibrium with $L^{a'}$ and L^b in equilibrium with $L^{b'}$) resulting in the generation of a dynamic "in situ" library,[22] with up to 10 different species theoretically present in solution: RhL^aL^a, $RhL^aL^{a'}$, $RhL^{a'}L^{a'}$, RhL^bL^b, $RhL^bL^{b'}$, $RhL^{b'}L^{b'}$, RhL^aL^b, $RhL^aL^{b'}$, $RhL^{a'}L^b$, $RhL^{a'}L^{b'}$. Although each species could, in principle, be present and catalyse the reaction, one of them could overcome the others, determining the direction and the extent of the enantioselectivity.

Herein, we report a full account on our results in the Rh-catalyzed asymmetric hydrogenation of prochiral olefins (dehydroamino acid derivatives, enamides and dimethyl itaconate) using a dynamic library of chiral phosphorus ligands containing a flexible (tropos) biphenol unit.[13]

Results and Discussion

Synthesis of the ligands: Biphenolic phosphites and phosphoramidites display several potential sites of diversity (R, R^1, R^2, R^3) and their preparation can be readily accomplished through a modular two-step synthesis (Scheme 2).[23,24]

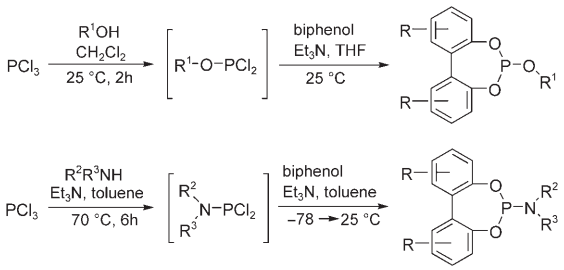

Scheme 2. Synthesis of the phosphorus ligands.

For the synthesis of phosphites [**1**-$P(O)_2O$–**11**-$P(O)_2O$] (Figure 1), the alcohol was treated at room temperature with PCl_3 in dichloromethane, followed by the slow addition of a solution of biphenol in tetrahydrofuran (Scheme 2). The reaction mixtures were purified by flash chromatography to give the phosphites as white foamy solids. Phosphoramidites [**12**-$P(O)_2N$–**19**-$P(O)_2N$] (Figure 1) were synthesized by treatment of the appropriate chiral secondary amine with PCl_3 at 70 °C in toluene and in the presence of triethylamine (Scheme 2). After cooling to −78 °C, a solution of biphenol in toluene was slowly added. The resulting mixtures were slowly warmed to room temperature and then purified by flash chromatography to give the phosphoramidites as white powders (see Experimental Section for details).

A library of 19 ligands was readily synthesized, by using three different biphenol backbones, that is, biphenol, 3,3′,5,5′-tetramethylbiphenol and 3,3′,5,5′-tetra-*tert*-butylbiphenol, and either a chiral alcohol [**1**-$P(O)_2O$–**11**-$P(O)_2O$] or a chiral secondary amine [**12**-$P(O)_2N$–**19**-$P(O)_2N$] (Figure 1).

Rhodium-catalyzed asymmetric hydrogenation of N-acetyldehydroamino acid derivatives: The hydrogenation experiments were initially performed on methyl 2-acetamidoacrylate, by using a library of 16 ligands [eight phosphites, **1**-$P(O)_2O$–**8**-$P(O)_2O$ and eight phosphoramidites, **12**-$P(O)_2N$–**19**-$P(O)_2N$]. The hydrogenation reactions were carried out overnight at 1 bar hydrogen pressure, in dichloromethane, by using 1 mol% [$Rh(cod)_2BF_4$] and a total of 2 mol% li-

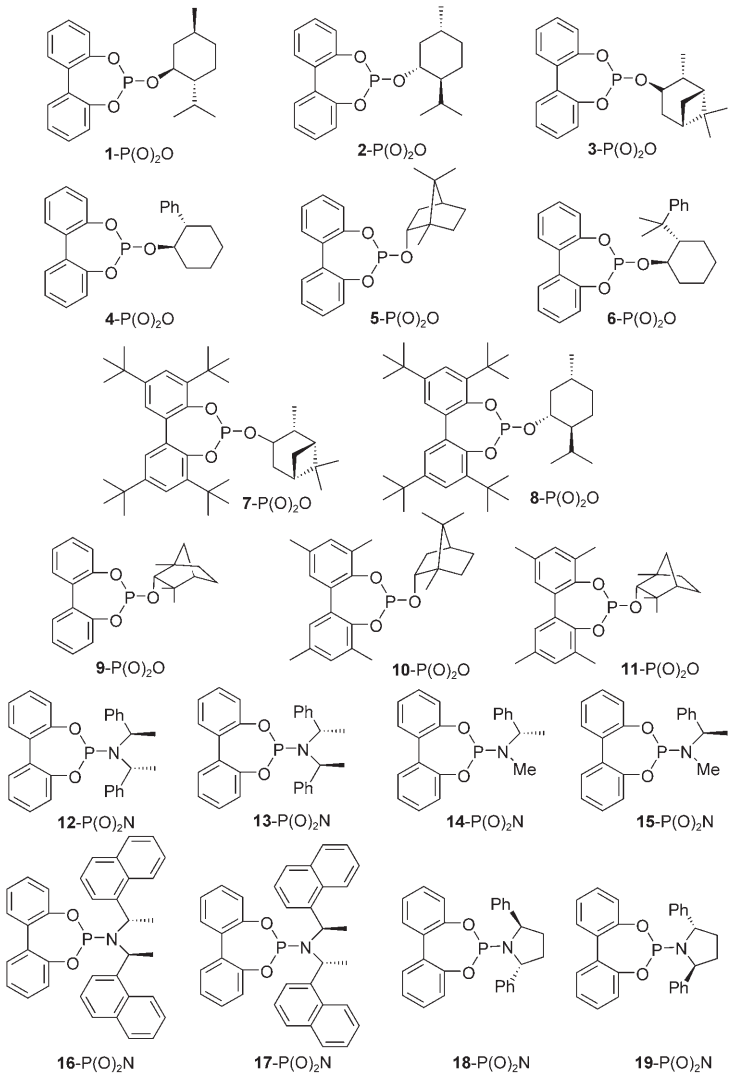

Figure 1. Library of 19 ligands, eleven phosphites [**1**-P(O)$_2$O–**11**-P(O)$_2$O] and eight phosphoramidites [**12**-P(O)$_2$N–**19**-P(O)$_2$N].

gands. The ligands were first screened individually (homocombinations, Table 1): in general, the phosphites were much more reactive than the phosphoramidites, allowing for excellent yields (up to 100%) and moderate enantiomeric excesses [up to 55%, entry 5, **5**-P(O)$_2$O].

By using combinations of two different ligands, 85 reactions were performed. Selected results are shown in Table 2 (entries 1–4), while further details can be found in the Supporting Information. By mixing two phosphoramidite ligands (see the Supporting Information), the hydrogenation product was generally obtained in moderate *ee* (lower than with the corresponding homocombinations), and poor conversion. The phosphite–phosphite combinations (see the Supporting Information) gave the product quantitatively, but with poor *ee* values. The phosphite/phosphoramidite combinations were the most productive, retaining the phosphite high reactivity (resulting in high conversions) and often improving the enantioselectivities compared with the

Table 1. Rh-catalyzed hydrogenation of methyl 2-acetamidoacrylate (ligand homocombinations).[a]

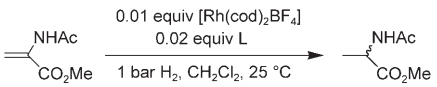

Entry	Ligand	Yield [%]	*ee* [%]	Abs. config.
1	**1**-P(O)$_2$O	100	11	*S*
2	**2**-P(O)$_2$O	100	11	*R*
3	**3**-P(O)$_2$O	100	25	*R*
4	**4**-P(O)$_2$O	80	53	*S*
5	**5**-P(O)$_2$O	100	55	*R*
6	**6**-P(O)$_2$O	100	48	*R*
7	**7**-P(O)$_2$O	100	0	–
8	**8**-P(O)$_2$O	100	36	*S*
9	**12**-P(O)$_2$N	7	52	*R*
10	**13**-P(O)$_2$N	7	52	*S*
11	**14**-P(O)$_2$N	100	44	*S*
12	**15**-P(O)$_2$N	100	44	*R*
13	**16**-P(O)$_2$N	15	0	–
14	**17**-P(O)$_2$N	15	0	–
15	**18**-P(O)$_2$N	30	13	*S*
16	**19**-P(O)$_2$N	30	13	*R*

[a] Reaction conditions: ligand (0.004 mmol), [Rh(cod)$_2$BF$_4$] (0.002 mmol), methyl 2-acetamidoacrylate (0.2 mmol), CH_2Cl_2 (2.0 mL), H_2 (1 bar), RT, 60 h. Yields and *ee* values were determined by GC equipped with a chiral capillary column (MEGADEX DACTBSβ, diacetyl-*tert*-butylsilyl-β-cyclodextrin) by using *n*-tridecane as internal standard.

homocombinations. The best combination **4**-P(O)$_2$O/**13**-P(O)$_2$N (entry 1) gave (*S*)-*N*-acetylalanine methyl ester in 87% *ee* (100% yield), while the corresponding mismatched combination [**4**-P(O)$_2$O/**12**-P(O)$_2$N, entry 4] gave (*R*)-*N*-acetylalanine methyl ester in 35% *ee* (100% yield). The amount of cooperation of these two ligands in the matched heterocombination is remarkable: the product *ee* is increased by some 34–35% compared to the corresponding homocombinations (see Figure 2), which is a much more pronounced increment than those usually observed by Reetz and Feringa in their studies.[5,6] The effect of the solvent[4e] was then studied and it was noticed that the use of more polar solvents (THF, EtOAc, alcohols) was beneficial to the enantioselectivity of the reaction (Table 2, entries 5–9); in particular, when isopropanol was used, the product was obtained in 94% *ee* and 100% yield (entry 7).

Selected heterocombinations were also tested in the hydrogenation of 2-acetamidoacrylic acid: under the optimized conditions (*i*PrOH, room temperature, 1 bar hydrogen pressure, overnight) the combination of ligands **4**-P(O)$_2$O and **13**-P(O)$_2$N gave (*S*)-*N*-acetylalanine in 94% *ee* and 100% yield (Table 3, entry 6; see also Figure 2).

We then decided to upgrade the library to nineteen ligands, with three new phosphites [**9**-P(O)$_2$O, **10**-P(O)$_2$O, **11**-P(O)$_2$O], and to screen it in the hydrogenation of methyl 2-acetamidocinnamate. The library screening was performed with a Premex-96 Multi reactor.[25] 94 Hydrogenation reactions were performed in parallel at room temperature in dichloromethane with 10 bar hydrogen pressure: 14 homocombinations (enantiomeric ligands were screened only once) and 80 heterocombinations. The combinations involving either two phosphites or two phosphoramidites were not

Table 2. Selected results of the Rh-catalyzed hydrogenation of methyl 2-acetamidoacrylate (ligand heterocombinations).[a]

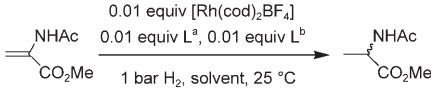

Entry	L^a	L^b	Solvent	Yield [%]	*ee* [%]	Abs. config.
1	**4**-P(O)$_2$O	**13**-P(O)$_2$N	CH_2Cl_2	100	87	*S*
2	**3**-P(O)$_2$O	**13**-P(O)$_2$N	CH_2Cl_2	40	73	*S*
3	**1**-P(O)$_2$O	**12**-P(O)$_2$N	CH_2Cl_2	50	72	*R*
4	**4**-P(O)$_2$O	**12**-P(O)$_2$N	CH_2Cl_2	100	35	*R*
5	**4**-P(O)$_2$O	**13**-P(O)$_2$N	MeOH	100	88	*S*
6	**4**-P(O)$_2$O	**13**-P(O)$_2$N	EtOH	100	89	*S*
7	**4**-P(O)$_2$O	**13**-P(O)$_2$N	*i*PrOH	100	94	*S*
8	**4**-P(O)$_2$O	**13**-P(O)$_2$N	EtOAc	100	91	*S*
9	**4**-P(O)$_2$O	**13**-P(O)$_2$N	THF	100	88	*S*

[a] Reaction conditions: ligands (0.002 mmol L^a and 0.002 mmol L^b), [Rh(cod)$_2$BF$_4$](0.002 mmol), methyl 2-acetamidoacrylate (0.2 mmol), solvent (2.0 mL), H_2 (1 bar), RT, 60 h. Yields and *ee* values were determined by GC equipped with a chiral capillary column (MEGADEX DACTBSβ diacetyl-*tert*-butylsilyl-β-cyclodextrin) by using *n*-tridecane as internal standard.

Table 3. Rh-catalyzed hydrogenation of 2-acetamidoacrylic acid.[a]

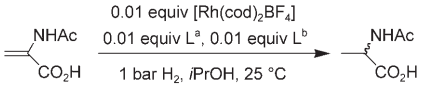

Entry	L^a	L^b	Yield [%]	*ee* [%]	Abs. config.
1	**3**-P(O)$_2$O	**3**-P(O)$_2$O	100	37	*R*
2	**4**-P(O)$_2$O	**4**-P(O)$_2$O	100	48	*S*
3	**13**-P(O)$_2$N	**13**-P(O)$_2$N	90	65	*S*
4	**14**-P(O)$_2$N	**14**-P(O)$_2$N	100	22	*S*
5	**4**-P(O)$_2$O	**13**-P(O)$_2$N	100	92	*S*
6[b]	**4**-P(O)$_2$O	**13**-P(O)$_2$N	100	94	*S*
7	**4**-P(O)$_2$O	**14**-P(O)$_2$N	90	46	*S*
8	**3**-P(O)$_2$O	**14**-P(O)$_2$N	100	92	*S*

[a] Reaction conditions: ligands (0.002 mmol L^a and 0.002 mmol L^b), [Rh(cod)$_2$BF$_4$] (0.002 mmol), 2-acetamidoacrylic acid (0.2 mmol), *i*PrOH (2.0 mL), H_2 (1 bar), RT, 60 h. Yields and *ee* values were determined by GC equipped with a chiral capillary column (MEGADEX DACTBSβ diacetyl-*tert*-butylsilyl-β-cyclodextrin) by using *n*-tridecane as internal standard, after treatment with a 2 M solution of trimethylsilyl diazomethane in Et_2O. [b] Substrate/rhodium 50:1.

Table 4. Selected examples of Rh-catalyzed hydrogenation of methyl 2-acetamidocinnamate.[a]

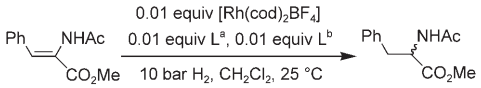

Entry	L^a	L^b	Conv. [%]	*ee* [%]	Abs. config.
1	**4**-P(O)$_2$O	**4**-P(O)$_2$O	100	64	*S*
2	**5**-P(O)$_2$O	**5**-P(O)$_2$O	100	51	*R*
3	**6**-P(O)$_2$O	**6**-P(O)$_2$O	100	19	*R*
4	**13**-P(O)$_2$N	**13**-P(O)$_2$N	2	6	*S*
5	**14**-P(O)$_2$N	**14**-P(O)$_2$N	100	39	*S*
6	**18**-P(O)$_2$N	**18**-P(O)$_2$N	73	31	*S*
7	**4**-P(O)$_2$O	**13**-P(O)$_2$N	82	85	*S*
8	**4**-P(O)$_2$O	**14**-P(O)$_2$N	100	54	*S*
9	**5**-P(O)$_2$O	**19**-P(O)$_2$N	100	69	*R*
10	**6**-P(O)$_2$O	**19**-P(O)$_2$N	100	64	*R*

[a] Reaction conditions: ligands (0.0035 mmol L^a and 0.0035 mmol L^b) [Rh(cod)$_2$BF$_4$] (0.0035 mmol), methyl 2-acetamidocinnamate (0.175 mmol), CH_2Cl_2 (2.5 mL) H_2 (10 bar), RT, 16 h. Conversions and *ee* values were determined by GC equipped with a chiral capillary column (CP-Chirasil-L-Val).

screened, on the basis of the limited reactivity and/or enantioselectivity showed by these combinations in the case of methyl 2-acetamidoacrylate. Selected results are shown in Table 4; further details of the results can be found in the Supporting Information. The homocombinations gave results ranging from 6% *ee* and 2% conversion [entry 4, **13**-P(O)$_2$N] to 64% *ee* and 100% conversion [entry 1, **4**-P(O)$_2$O]. The best result was obtained with the heterocombination of ligands **4**-P(O)$_2$O and **13**-P(O)$_2$N, allowing for 85% *ee* and 82% conversion (Table 4, entry 7). Also in this case the *ee* increment obtained by the use of the ligand heterocombination compared to the corresponding homocombinations is quite remarkable (see Figure 3).

The solvent screening was carried out by using a multireactor autoclave (Argonaut Endeavor) that allows eight reactions to be run in parallel: in particular, isopropanol allowed for 95% *ee* and 100% conversion at 5 bar hydrogen pressure (entry 3, Table 5).

The best heterocombinations [**4**-P(O)$_2$O/**13**-P(O)$_2$N, **5**-P(O)$_2$O/**19**-P(O)$_2$N and **6**-P(O)$_2$O/**19**-P(O)$_2$N] and the corresponding homocombinations identified in the hydrogenation of methyl 2-acetamidocinnamate were also screened for the hydrogenation of 2-acetamidocinnamic acid (Table 6) and excellent results were obtained with the combination **4**-P(O)$_2$O/**13**-P(O)$_2$N (93% *ee*, 100% conversion, entry 6; see also Figure 3).

Substituted 2-acetamidocinnamic acids were then tested by using the heterocombination **4**-P(O)$_2$O and **13**-P(O)$_2$N (Table 7). The introduction of a Cl substituent in the phenyl ring resulted in a significant increase of the enantioselectivity: with both *N*-acetyl-2-chlorodehydrophenylalanine and *N*-acetyl-4-chlorodehydrophenylalanine as substrates, excellent enantioselectivities (98–97% *ee*) and quantitative conversions were obtained in *i*PrOH (Table 7, entries 3 and 9; see also Figure 4).

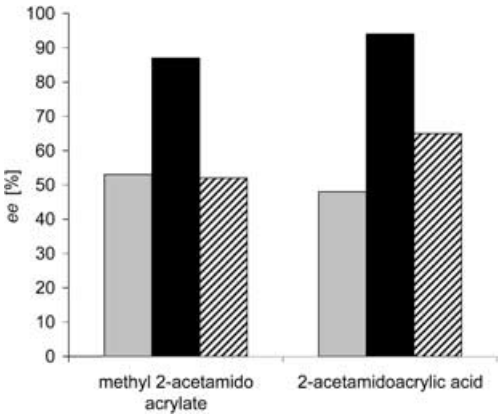

Figure 2. Best ligand heterocombination and corresponding ligand homocombinations for the hydrogenation of 2-acetamidoacrylic acid and methyl ester: ■ [**4**-$P(O)_2O]_2$, ■ **4**-$P(O)_2O$/**13**-$P(O)_2N$, /// [**13**-$P(O)_2N]_2$.

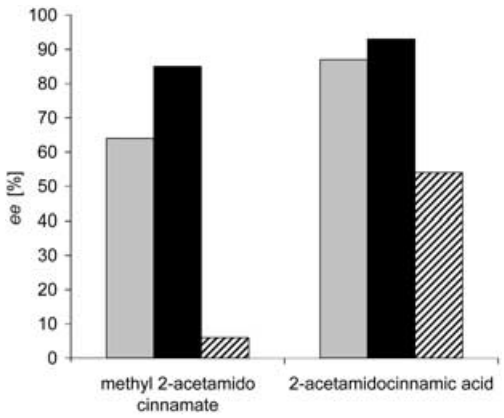

Figure 3. Best ligand heterocombination and corresponding ligand homocombinations for the hydrogenation of 2-acetamidocinnamic acid and methyl ester: ■ [**4**-$P(O)_2O]_2$, ■ **4**-$P(O)_2O$/**13**-$P(O)_2N$, /// [**13**-$P(O)_2N]_2$.

Table 5. Reaction conditions optimization for the best heterocombination of Rh-catalyzed hydrogenation of methyl 2-acetamidocinnamate.[a]

Entry	L^a	L^b	Solvent	H_2 [bar]	Conv. [%]	*ee* [%]	Abs. config.
1	**4**-$P(O)_2O$	**13**-$P(O)_2N$	CH_2Cl_2	10	82	85	*S*
2	**4**-$P(O)_2O$	**13**-$P(O)_2N$	*i*PrOH	10	98	92	*S*
3	**4**-$P(O)_2O$	**13**-$P(O)_2N$	*i*PrOH	5	100	95	*S*
4	**4**-$P(O)_2O$	**13**-$P(O)_2N$	EtOAc	10	67	88	*S*

[a] Reaction conditions: ligands (0.01 mmol L^a and 0.01 mmol L^b), $[Rh(cod)_2BF_4]$ (0.01 mmol), methyl 2-acetamidocinnamate (0.5 mmol), solvent (5.0 mL), H_2 (5–10 bar), RT, 90 min. Conversions and *ee* values were determined by GC equipped with a chiral capillary column (CP-Chirasil-L-Val).

Table 6. Rh-catalyzed hydrogenation of 2-acetamidocinnamic acid.[a]

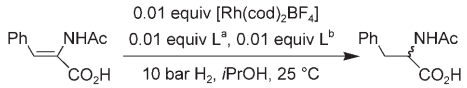

Entry	L^a	L^b	Conv. [%]	*ee* [%]	Abs. config.
1	**4**-$P(O)_2O$	**4**-$P(O)_2O$	100	87	*S*
2	**5**-$P(O)_2O$	**5**-$P(O)_2O$	100	31	*R*
3	**6**-$P(O)_2O$	**6**-$P(O)_2O$	100	8	*R*
4	**13**-$P(O)_2N$	**13**-$P(O)_2N$	83	54	*S*
5	**19**-$P(O)_2N$	**19**-$P(O)_2N$	100	14	*R*
6	**4**-$P(O)_2O$	**13**-$P(O)_2N$	100	93	*S*
7	**5**-$P(O)_2O$	**19**-$P(O)_2N$	100	18	*R*
8	**6**-$P(O)_2O$	**19**-$P(O)_2N$	100	10	*R*

[a] Reaction conditions: ligands (0.01 mmol L^a and 0.01 mmol L^b), $[Rh(cod)_2BF_4]$ (0.01 mmol), methyl 2-acetamidocinnamate (0.5 mmol), *i*PrOH (5.0 mL), H_2 (10 bar), RT, 24 h. Conversions and *ee* values were determined by chiral HPLC (Chirobiotic T).

The enantioselectivity decreases very modestly with increasing pressure (cf. entries 3 and 4), while the solvent has a dramatic effect on the outcome of the reaction: the activity of the catalyst is depressed in dichloromethane (entries 5 and 10), possibly due to the poor solubility of the substrates, while in methanol the *ee* values are decreased (entries 6 and 11).

The enantioselective hydrogenation of β-acylamino acrylates[4k] gives access to chiral β-amino acid derivatives which are important pharmaceutical building blocks. For this reason, the ligand library was screened in the hydrogenation of methyl (*Z*)-3-acetamidocrotonate. Preliminary tests were performed by using the Argonaut Endeavor multireactor autoclave: eight reactions were run in parallel, in isopropanol as solvent, with a single ligand in each vessel (homocombinations) (Table 8).

The enantioselectivities were modest, nonetheless we decided to perform a more comprehensive screening, including 80 heterocombinations, by using a 96-Multi Reactor (see Supporting Information). Stock solutions of the ligands and $[Rh(cod)_2BF_4]$ were prepared in dichloromethane, while the substrate was dissolved in *i*PrOH; the reactions were thus performed in 1:3 dichloromethane/*i*PrOH. Enantioselectivities were still only moderate (up to 45% *ee*; see the Supporting Information for further details of the screening); better results were obtained in pure *i*PrOH (Table 9). It is worth noting that the effect of the solvent on both enantioselectivity and conversion is not always consistent. For example, *i*PrOH turned out to be the best solvent, leading to 71% *ee* for the heterocombination **3**-$P(O)_2O$/**19**-$P(O)_2N$ (Table 9 entry 3; see also Figure 5) and to 69% *ee* for the heterocombination **9**-$P(O)_2O$/**19**-$P(O)_2N$ (entry 10), where *i*PrOH/CH_2Cl_2 resulted in lower conversions and enantioselectivities (Table 9, entries 2 vs 3, and 9 vs 10). In other cases [**5**-$P(O)_2O$/**18**-$P(O)_2N$ and **9**-$P(O)_2O$/**15**-$P(O)_2N$], this trend was reverted

Table 7. Rh-catalyzed hydrogenation of substituted 2-acetamidocinnamic acid.[a]

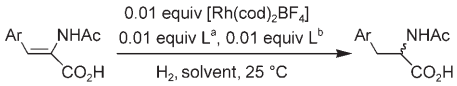

Entry	Ar	L^a	L^b	pH_2 [bar]	Solvent	Conv. [%]	*ee* [%]	Abs. config.
1	2-Cl-C_6H_4	**4**-$P(O)_2O$	**4**-$P(O)_2O$	10	*i*PrOH	100	89	*S*
2	2-Cl-C_6H_4	**13**-$P(O)_2N$	**13**-$P(O)_2N$	10	*i*PrOH	34	72	*S*
3	2-Cl-C_6H_4	**4**-$P(O)_2O$	**13**-$P(O)_2N$	10	*i*PrOH	100	98	*S*
4	2-Cl-C_6H_4	**4**-$P(O)_2O$	**13**-$P(O)_2N$	25	*i*PrOH	100	95	*S*
5	2-Cl-C_6H_4	**4**-$P(O)_2O$	**13**-$P(O)_2N$	10	CH_2Cl_2	0	–	–
6	2-Cl-C_6H_4	**4**-$P(O)_2O$	**13**-$P(O)_2N$	10	MeOH	100	89	*S*
7	4-Cl-C_6H_4	**4**-$P(O)_2O$	**4**-$P(O)_2O$	10	*i*PrOH	100	88	*S*
8	4-Cl-C_6H_4	**13**-$P(O)_2N$	**13**-$P(O)_2N$	10	*i*PrOH	16	56	*S*
9	4-Cl-C_6H_4	**4**-$P(O)_2O$	**13**-$P(O)_2N$	10	*i*PrOH	100	97	*S*
10	4-Cl-C_6H_4	**4**-$P(O)_2O$	**13**-$P(O)_2N$	10	CH_2Cl_2	0	–	–
11	4-Cl-C_6H_4	**4**-$P(O)_2O$	**13**-$P(O)_2N$	10	MeOH	98	67	*S*

[a] Reaction conditions: ligands (0.01 mmol L^a and 0.01 mmol L^b), $[Rh(cod)_2BF_4]$ (0.01 mmol), substrate (0.5 mmol), solvent (5.0 mL), H_2 (10–25 bar), 90 min. Conversions and *ee* values were determined by chiral HPLC (Chirobiotic T).

Table 8. Rh-catalyzed hydrogenation of methyl (*Z*)-3-acetamidocrotonate.[a]

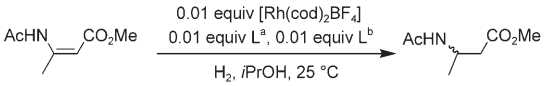

Entry	Ligand ($L^a = L^b$)	Substrate/Rh	pH_2 [bar]	Conv. [%]	*ee* [%]	Abs. config.
1	**1**-$P(O)_2O$	50	10	93	1	*R*
2	**4**-$P(O)_2O$	50	10	100	31	*S*
3	**5**-$P(O)_2O$	50	10	100	6	*R*
4	**9**-$P(O)_2O$	20	25	100	26	*R*
5	**11**-$P(O)_2O$	50	10	100	9	*S*
6	**12**-$P(O)_2N$	50	10	0	–	–
7	**19**-$P(O)_2N$	50	10	79	1	*R*
8	**19**-$P(O)_2N$	20	25	62	12	*R*

[a] Reaction conditions: ligand ($L^a = L^b = 0.02$ mmol), $[Rh(cod)_2BF_4]$ (0.01 mmol), methyl (*Z*)-3-acetamidocrotonate (0.2–0.5 mmol), solvent (5.0 mL), H_2 (10–25 bar), 90 min. Conversions and *ee* values were determined by GC equipped with a chiral capillary column (CP-Chirasil-Dex-CB).

Table 9. Solvent screening for the hydrogenation of methyl (*Z*)-3-acetamidocrotonate.[a]

Entry	L^a	L^b	Solvent	Conv. [%]	*ee* [%]	Abs. config.
1	**5**-$P(O)_2O$	**19**-$P(O)_2N$	*i*PrOH/CH_2Cl_2	100	45	*R*
2	**3**-$P(O)_2O$	**19**-$P(O)_2N$	*i*PrOH/CH_2Cl_2	100	43	*R*
3	**3**-$P(O)_2O$	**19**-$P(O)_2N$	*i*PrOH	100	71	*R*
4	**5**-$P(O)_2O$	**18**-$P(O)_2N$	*i*PrOH/CH_2Cl_2	100	35	*S*
5	**5**-$P(O)_2O$	**18**-$P(O)_2N$	*i*PrOH	100	14	*S*
6	**9**-$P(O)_2O$	**15**-$P(O)_2N$	CH_2Cl_2	43	50	*R*
7	**9**-$P(O)_2O$	**15**-$P(O)_2N$	*i*PrOH/CH_2Cl_2	100	34	*R*
8	**9**-$P(O)_2O$	**15**-$P(O)_2N$	*i*PrOH	100	18	*R*
9	**9**-$P(O)_2O$	**19**-$P(O)_2N$	*i*PrOH/CH_2Cl_2	100	41	*R*
10	**9**-$P(O)_2O$	**19**-$P(O)_2N$	*i*PrOH	100	69	*R*

[a] Reaction conditions: ligands (0.0035 mmol L^a and 0.0035 mmol L^b), $[Rh(cod)_2BF_4]$ (0.0035 mmol), methyl (*Z*)-3-acetamidocrotonate (0.175 mmol), solvent (2.5 mL), H_2 (25 bar), RT, 16 h. Conversions and *ee* values were determined by GC equipped with a chiral capillary column (CP-Chirasil-Dex-CB).

and better results were obtained in *i*PrOH/CH_2Cl_2 3:1 or pure dichloromethane (Table 9, entries 4–5, 6–8).

Kinetic studies and improvement of the heterocombination ligand ratio: The remarkable increase of *ee* which was obtained with the heterocombinations compared with the single ligands promted us to try to shed some light into the "black box" of this ligand system. A comparison of the rates of the hydrogenation of methyl 2-acetamidocinnamate by using single ligands **4**-$P(O)_2O$ and **13**-$P(O)_2N$ and their heterocombination is displayed in Figure 6. These traces represent the hydrogen uptake during the hydrogenation, at 5 bar pressure in *i*PrOH, performed simultaneously by using the Argonaut Endeavor multireactor autoclave which allows continuous monitoring of the hydrogen uptake for eight parallel reactions.

Phosphite **4**-$P(O)_2O$ proved to be the most active with full conversion whithin 30 minutes (with 79% *ee*). The reaction seemingly follows a zero-order kinetic law.[26] In the case of phosphoramidite **13**-$P(O)_2N$, the hydrogenation was much slower, giving poor conversion even after 5 h at 5 bar hydrogen pressure (3% conversion, 36% *ee*). When the 1:1 heterocombination of ligands **4**-$P(O)_2O$ and **13**-$P(O)_2N$ was employed, the reaction was definitely slower than the phosphite-catalyzed reaction and apparently follows a first-order kinetic law. However, as expected, the highest enantioselectivity (95% *ee*) was obtained with complete conversion in 2 h.

As we anticipated in the introduction, the use of a combination of two ligands (L^a and L^b) should result in the generation of a dynamic "in situ" library, with several, different, catalytically active species, simultaneously present in the reaction medium. On the basis of this assumption, we envisaged that, by modifying the L^a/L^b ratio, we could influence the concentration of the different species and possibly the stereochemical outcome of the reaction. In particular, we speculated that lowering the ratio **4**-$P(O)_2O$/**13**-$P(O)_2N$, but keeping constant the ($L^a + L^b$)/Rh ratio (equal to 2), less rhodium complex containing only **4**-$P(O)_2O$ (very active,

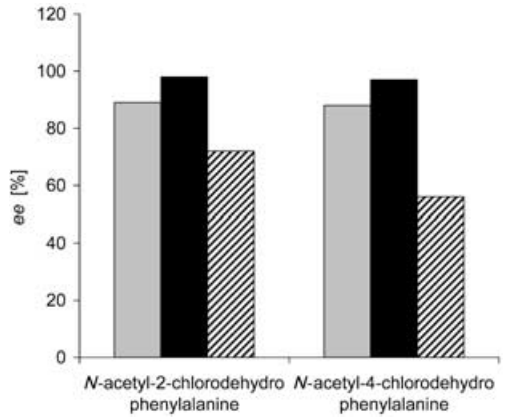

Figure 4. Best ligand heterocombination and corresponding ligand homocombinations for the hydrogenation of *N*-acetyl-2-chlorodehydrophenylalanine and *N*-acetyl-4-chlorodehydrophenylalanine: ■ [**4**-P(O)$_2$O]$_2$, ■ **4**-P(O)$_2$O/**13**-P(O)$_2$N, /// [**13**-P(O)$_2$N]$_2$.

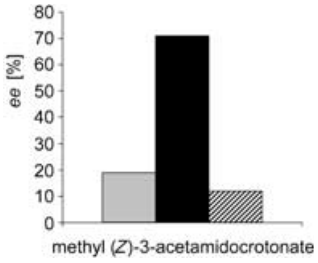

Figure 5. Best ligand heterocombination and corresponding ligand homocombinations for the hydrogenation of methyl (*Z*)-3-acetamidocrotonate: ■ [**3**-P(O)$_2$O]$_2$, ■ **3**-P(O)$_2$O/**19**-P(O)$_2$N, /// [**19**-P(O)$_2$N]$_2$.

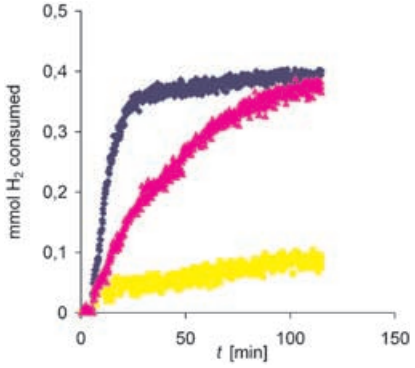

Figure 6. Hydrogen uptake in the hydrogenation of methyl 2-acetamidocinnamate at 5 bar in *i*PrOH, by using **4**-P(O)$_2$O (◆), **13**-P(O)$_2$N (■), and a 1:1 combination of **4**-P(O)$_2$O and **13**-P(O)$_2$N (▲).

but less enantioselective) would be present in solution. This would in turn favour the concentration of mixed complexes containing both **4**-P(O)$_2$O and **13**-P(O)$_2$N, apparently the most selective ones. The species containing only **13**-P(O)$_2$N would become predominant but, being almost not-active, should not influence significantly the reaction outcome. To confirm this hypothesis, a model was considered, by using ligands **6**-P(O)$_2$O and **12**-P(O)$_2$N for the hydrogenation of methyl 2-acetamidocinnamate, for which we knew that only moderate enantioselectivities had been obtained during the library screening. In fact, phosphite **6**-P(O)$_2$O gave the hydrogenation product with full conversion and 21% *ee*; phosphoramidite **12**-P(O)$_2$N gave only 2% conversion and 30% *ee*, and the 1:1 combination of **6**-P(O)$_2$O and **12**-P(O)$_2$N allowed for 100% conversion and 34% *ee*. When a 0.25 to 1.75 of **6**-P(O)$_2$O and **12**-P(O)$_2$N was employed, the enantioselectivity of the reaction increased to 59% *ee* (40% conversion). Encouraged by these results, we applied the same principle to the best heterocombination: **4**-P(O)$_2$O and **13**-P(O)$_2$N. A screening of the relative ratio of the two ligands was carried out, keeping constant the (L^a+L^b)/Rh ratio (equal to 2) (Figure 7). The best L^a/L^b ratio identified was

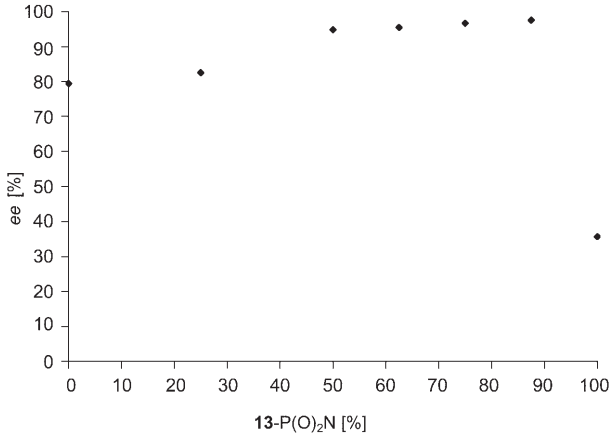

Figure 7. Dependence of the product *ee* on the ratio **4**-P(O)$_2$O/**13**-P(O)$_2$N for the hydrogenation of methyl 2-acetamidocinnamate at 5 bar, in *i*PrOH.

0.25 to 1.75 for **4**-P(O)$_2$O and **13**-P(O)$_2$N, respectively, which gave the hydrogenation product in 98% *ee* and 79% conversion (79% *ee* and 100% conversion with **4**-P(O)$_2$O; 36% *ee* and 2% conversion with and **13**-P(O)$_2$N; 95% *ee* and 100% conversion with a 1:1 ratio of **4**-P(O)$_2$O/**13**-P(O)$_2$N).

The same study was then performed for the hydrogenation of methyl 2-acetamidoacrylate. The kinetic curves for, respectively, the homocombination of phosphite **4**-P(O)$_2$O, the homocombination of phosphoramidite **13**-P(O)$_2$N and the heterocombination of these two ligands (the best combination identified) were compared (Figure 8). The hydrogen uptake profile of the heterocombination was quite similar to the homocombination of the phosphite, and resembles a zero-order kinetic law.[26] In this case the reaction with the heterocombination of ligands is faster and a complete conversion was observed within 20 min.

When the screening of the relative ratio of the two ligands was performed, similar trends to those identified in the hydrogenation of methyl 2-acetamidocinnamate were observed (Figure 9). The best L^a/L^b ratio identified was again 0.25 to 1.75 for **4**-P(O)$_2$O and **13**-P(O)$_2$N, respectively, allowing for

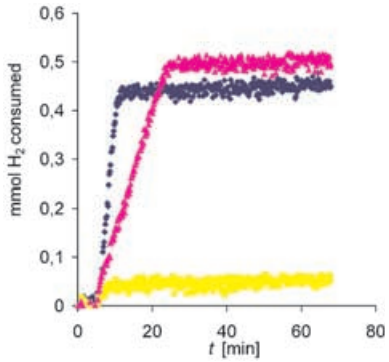

Figure 8. Hydrogen uptake in the hydrogenation of methyl 2-acetamidoacrylate at 5 bar in *i*PrOH, by using **4**-$P(O)_2O$ (◆), **13**-$P(O)_2N$ (■), and a 1:1 combination of **4**-$P(O)_2O$ and **13**-$P(O)_2N$ (▲).

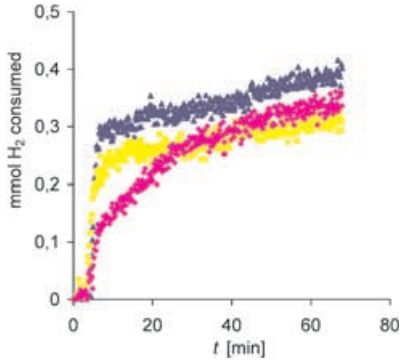

Figure 10. Hydrogen uptake in the hydrogenation of methyl (*Z*)-3-acetamidocrotonate at 5 bar in *i*PrOH, by using **3**-$P(O)_2O$ (▲), **19**-$P(O)_2N$ (■), and a 1:1 combination of **3**-$P(O)_2O$ and **19**-$P(O)_2N$ (◆).

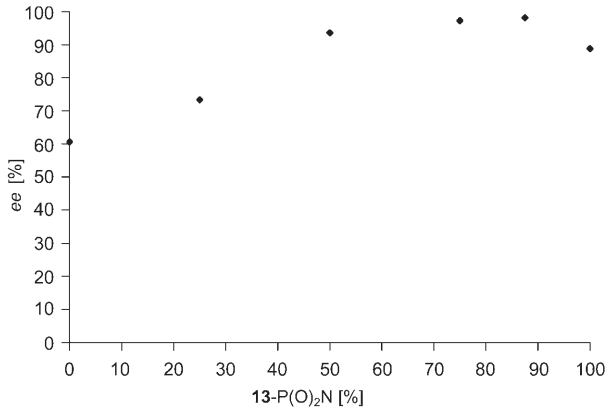

Figure 9. Dependence of the product *ee* on the ratio **4**-$P(O)_2O$/**13**-$P(O)_2N$ for the hydrogenation of methyl 2-acetamidoacrylate at 5 bar, in *i*PrOH.

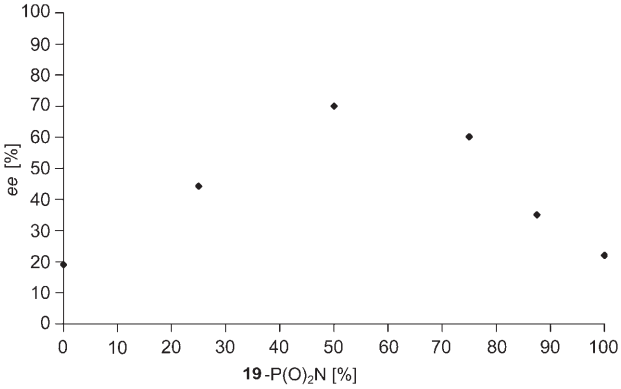

Figure 11. Dependence of the product *ee* on the ratio **3**-$P(O)_2O$/**19**-$P(O)_2N$ for the hydrogenation of methyl (*Z*)-3-acetamidocrotonate at 25 bar, in *i*PrOH.

98% *ee* and 100% conversion (61% *ee* and 100% conversion with **4**-$P(O)_2O$; 89% *ee* and 3% conversion with **13**-$P(O)_2N$; 94% *ee* and 100% conversion with a 1 to 1 ratio of **4**-$P(O)_2O$ and **13**-$P(O)_2N$).

When the rates of the hydrogenation of methyl (*Z*)-3-acetamidocrotonate by using ligands **3**-$P(O)_2O$, **19**-$P(O)_2N$ and their heterocombination were measured by hydrogen uptake, a different behaviour was displayed (Figure 10). In this case, phosphoramidite **19**-$P(O)_2N$ gives rise to a very active catalyst, that allows for full conversion within 1 h, while the reaction performed by using the heterocombination is slower although more enantioselective.

This result was confirmed by the study of the relative ratio of the two ligands, in *i*PrOH at 25 bar hydrogen pressure (Figure 11), which showed that the 1:1 ratio **3**-$P(O)_2O$/**19**-$P(O)_2N$ was the most effective, both in terms of enantioselectivity and conversion (71% *ee*, 100% conversion). An excess of either one of the two ligands reduces the overall enantioselectivity (19% *ee* and 100% conversion with **3**-$P(O)_2O$; 22% *ee* and 91% conversion with and **19**-$P(O)_2N$; 60% *ee* and 83% conversion with a 0.5:1.5 ratio **3**-$P(O)_2O$/**19**-$P(O)_2N$).

Rhodium-catalyzed asymmetric hydrogenation of enamides: Asymmetric hydrogenation of arylalkylenamides such as **20** and **21**[4m] (Figure 12) gives access to enantiomerically enriched arylalkylamines, which are particularly interesting building blocks for pharmaceutical compounds and are extensively used in organic synthesis and catalysis (as resolving agents and chiral auxiliaries). These prochiral enamides were synthesized in two-steps from simple ketones.[27]

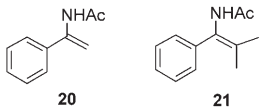

Figure 12. Enamide substrates.

A full screening (94 reactions performed in parallel) was carried out for the hydrogenation of enamide **20**, at 25 bar hydrogen pressure in dichloromethane (enamides are less reactive substrates than dehydroamino acid derivatives). Selected results are shown in Table 10, entries 1–6; further details can be found in the Supporting Information. The hydrogenation generally proceeded to completion, and the best result (85% *ee*, entry 1) was obtained in this case with a single phosphite ligand [**4**-$P(O)_2O$]. The hydrogenation of enamide **21**, carried out in a 96 Multireactor, at 25 bar hy-

Table 10. Selected results for the hydrogenation of enamides **20** and **21**.[a]

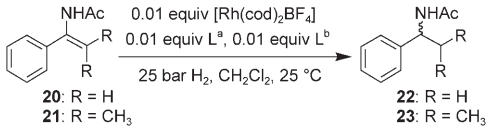

20: R = H
21: R = CH_3

22: R = H
23: R = CH_3

Entry	Substrate	L^a	L^b	Conv. [%]	*ee* [%]	Abs. config.
1	**20**	**4**-$P(O)_2O$	**4**-$P(O)_2O$	100	85	*S*
2	**20**	**11**-$P(O)_2O$	**11**-$P(O)_2O$	100	75	*S*
3	**20**	**1**-$P(O)_2O$	**18**-$P(O)_2N$	100	64	*S*
4	**20**	**4**-$P(O)_2O$	**13**-$P(O)_2N$	100	82	*S*
5	**20**	**4**-$P(O)_2O$	**16**-$P(O)_2N$	100	79	*S*
6	**20**	**8**-$P(O)_2O$	**14**-$P(O)_2N$	100	66	*S*
7	**21**	**1**-$P(O)_2O$	**18**-$P(O)_2N$	72	39	[b]
8	**21**	**8**-$P(O)_2O$	**12**-$P(O)_2N$	55	36[c]	[b]
9	**21**	**10**-$P(O)_2O$	**18**-$P(O)_2N$	100	38	[b]
10	**21**	**11**-$P(O)_2O$	**18**-$P(O)_2N$	100	47	[b]

[a] Reaction conditions: ligands (0.0035 mmol L^a and 0.0035 mmol L^b) $[Rh(cod)_2BF_4]$ (0.0035 mmol), substrate (0.175 mmol), CH_2Cl_2 (2.5 mL), H_2 (25 bar), RT, 16 h. Conversions and *ee* values were determined by GC equipped with a chiral capillary column (CP-Chirasil-L-Val). [b] Not determined. [c] The major enantiomer obtained in entry 8 has the opposite configuration in comparison to entries 7, 9, 10.

drogen pressure, in dichloromethane, proceeded slower than the hydrogenation of the less hindered enamide **20** (selected results are shown in Table 10, entries 7–10). However, running the hydrogenations overnight, moderate to good conversions were obtained in several cases. As for the *ee*, the heterocombination **11**-$P(O)_2O$/**18**-$P(O)_2N$ allowed for 47% *ee* (entry 10), which is a valuable result, considering that essentially no good monodentate ligand has ever been reported for tetrasubstituted enamides.

Rhodium-catalyzed asymmetric hydrogenation of dimethyl itaconate: The hydrogenation of dimethyl itaconate had previously been studied in great detail by using both mono- and bidentate ligands.[4m] A full screening (94 hydrogenation reactions performed in parallel) was performed at 10 bar hydrogen pressure in dichloromethane. Selected results are shown in Table 11, whereas further details can be found in the Supporting Information. With this substrate, the best result was obtained with a single phosphoramidite ligand (**18**-$P(O)_2N$ or its enantiomer **19**-$P(O)_2N$), allowing for 75% *ee* and 94% conversion (Table 11, entries 5, 6). Phosphite **6**-$P(O)_2O$ gave 74% *ee* and 90% conversion (Table 11, entry 2).[28,29]

Table 11. Selected results for the hydrogenation of dimethyl itaconate.[a]

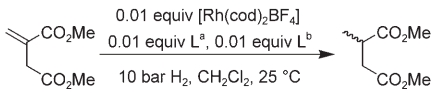

Entry	L^a	L^b	Conv. [%]	*ee* [%]	Abs. config.
1	**4**-$P(O)_2O$	**4**-$P(O)_2O$	25	69	*R*
2	**5**-$P(O)_2O$	**5**-$P(O)_2O$	100	46	*S*
3	**6**-$P(O)_2O$	**6**-$P(O)_2O$	90	74	*S*
4	**9**-$P(O)_2O$	**9**-$P(O)_2O$	100	60	*S*
5	**11**-$P(O)_2O$	**11**-$P(O)_2O$	100	72	*R*
6	**13**-$P(O)_2N$	**13**-$P(O)_2N$	0	–	–
7	**15**-$P(O)_2N$	**15**-$P(O)_2N$	79	3	*S*
8	**16**-$P(O)_2N$	**16**-$P(O)_2N$	3	2	*R*
9	**18**-$P(O)_2N$	**18**-$P(O)_2N$	94	75	*S*
10	**19**-$P(O)_2N$	**19**-$P(O)_2N$	94	75	*R*
11	**5**-$P(O)_2O$	**18**-$P(O)_2N$	100	63	*S*
12	**9**-$P(O)_2O$	**15**-$P(O)_2N$	100	59	*S*
13	**11**-$P(O)_2O$	**13**-$P(O)_2N$	62	66	*R*
14	**11**-$P(O)_2O$	**16**-$P(O)_2N$	40	61	*R*

[a] Reaction conditions: ligands (0.0035 mmol L^a and 0.0035 mmol L^b), $[Rh(cod)_2BF_4]$ (0.0035 mmol), dimethyl itaconate (0.175 mmol), CH_2Cl_2 (2.5 mL), H_2 (10 bar), RT, 16 h. Conversions and *ee* values were determined by GC equipped with a chiral capillary column (CP-Chirasil-L-Val).

A simple mathematical model for a better understanding of the variation of the enantiomeric excess with the ratio of $P(O)_2O/P(O)_2N$: Experiments have shown that by using a ratio $P(O)_2O/P(O)_2N$ different from 1:1 while keeping the $(L^a + L^b)$/Rh ratio equal to 2 can lead to a significant improvement of the *ee* of the hydrogenated products. A simple mathematical model was built to describe and better understand this phenomenon. This model is not a kinetic analysis in the sense that it does not use any kinetic laws nor does it rely on the reaction mechanism involved in the transformation.

Building the mathematical model: As long as the ratio ligands $[P(O)_2O + P(O)_2N]$ to Rh is kept equal to 2 and if we assume that Rh complexes bearing only one or more than two phosphorus ligands are not stable relatively to RhL_2 species, only three Rh complexes co-exist in equilibrium in solution.[30] Their inter-conversion is fully described by the following equation.

$$Rh[P(O)_2O]_2 + Rh[P(O)_2N]_2 \overset{K}{\rightleftarrows} 2\,Rh[P(O)_2O][P(O)_2N] \quad (1)$$

The equilibrium constant (K), allows us to estimate the relative amount of each of the three species in solution for various amounts of $P(O)_2O$ and $P(O)_2N$ initially used. K is, above all, dependent on the nature of the $P(O)_2O$ or $P(O)_2N$ ligands. Its value is unknown,[31] and thus constitutes a parameter to fit our model with the experimental data. Equation (1) leads to a characteristic distribution for the three different complexes at the equilibri-

um for different ratios of $P(O)_2O/P(O)_2N$ (see Figure 13). Note that in Figure 13 and all related subsequent figures, the *x* axis gives the amount of $P(O)_2O$ ligand to Rh. Considering that we kept the ligands to Rh ratio equal to 2, a value of 0 for $P(O)_2O$ amount is equivalent to a value of 2 for the $P(O)_2N$ amount. For any value of *K*, the maximum amount of hetero-complex is always obtained for a 1:1 mixture of $P(O)_2O/P(O)_2N$. Higher or lower values of *K* only cause the amplitude of the parabolic curve for the equilibrium amount of $Rh[P(O)_2O][P(O)_2N]$ (see △ in Figure 13) to vary. More importantly the ratio of $Rh[P(O)_2O][P(O)_2N]$ to $Rh[P(O)_2O]_2$ increases exponentially when the amount of $P(O)_2O$ is reduced (see × in Figure 13). In the case of a mixture of catalytic species all able to catalyze the same reaction, the ratio between these species is indeed the crucial parameter to consider and we can easily foresee, as it has been demonstrated experimentally, how a 1:1 mixture of ligands may not lead to the optimal catalytic mixture.

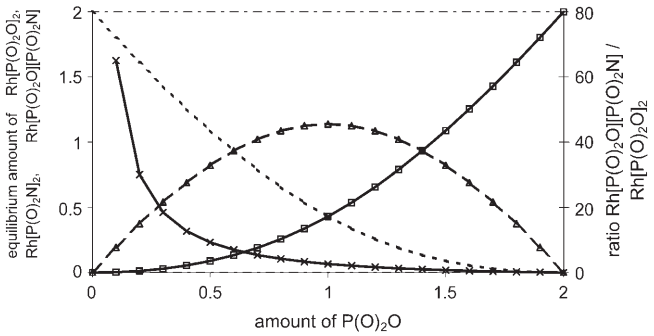

Figure 13. Amount of □: $Rh[P(O)_2O]_2$, -----: $Rh[P(O)_2N]_2$, △: $Rh[P(O)_2O][P(O)_2N]$ at the equilibrium vs amount of $P(O)_2O$ [$P(O)_2O$+$P(O)_2N$ kept constant, equal to 2], plotted for $K=7$, ×: ratio $Rh[P(O)_2O][P(O)_2N]/Rh[P(O)_2O]_2$.

The *ee* values obtained in asymmetric hydrogenation by using the mixtures of the three Rh complexes as catalysts can be calculated after making a few additional assumptions/simplifications concerning the hydrogenation rate and selectivity of each individual species:

- *for the $Rh[P(O)_2O]_2$ and $Rh[P(O)_2N]_2$ complexes*: As these species can be prepared cleanly, the rate and *ee* can be measured and are assumed to be the same in the mixtures. In our model, when we calculate the *ee* obtained with a mixture of $P(O)_2O$ and $P(O)_2N$, only the ratio between the rates of the three catalytic species present in solution is needed. We will consequently use relative rates (without unit). Moreover, we assume that these relative rates remain constant throughout the reaction. Based on the experimental data, we estimate the rate of the $Rh[P(O)_2O]_2$ complex to be approximately two orders of magnitude higher than of the $Rh[P(O)_2N]_2$ complex. For example, for the **4**-$P(O)_2O$/**13**-$P(O)_2N$ mixtures, the TOF of the homo-complexes are around 300 h^{-1} for the Rh[**4**-$P(O)_2O]_2$ and 0.6 h^{-1} for the Rh[**13**-$P(O)_2N]_2$. In our model, for example, the rate of Rh[**13**-$P(O)_2N]_2$ can then be arbitrarily set to 1, imposing the rate of Rh[**4**-$P(O)_2O]_2$ to be 500.
- *for the $Rh[P(O)_2O][P(O)_2N]$ complexes*: neither the rate, nor the *ee* of a pure $Rh[P(O)_2O][P(O)_2N]$ complex can be measured since the hetero-complex only exists in presence of both homo-complexes. Nevertheless, we can estimate that its rate is comparable to the one of the $Rh[P(O)_2O]_2$ complex otherwise it would not make a significant contribution to the observed *ee* values. Also, when considering cases where the mixture of ligands leads to an improvement, we can estimate the *ee* of the pure $Rh[P(O)_2O][P(O)_2N]$ complex to be at least equal or most probably better than the value of the observed improved *ee*.
- The three catalytic species are entirely selective towards the production of hydrogenated products and are not involved in side reactions leading to the formation of other products or to their own decomposition.

Knowing the distribution of the three catalytic species in solution based on *K* and their respectives rates and enantioselectivities, it is easy to calculate the *ee* according to a formula of the type below:

$$E(R) = f\{Rh[P(O)_2O]_2\} \cdot r\{Rh[P(O)_2O]_2\} \cdot S_R\{Rh[P(O)_2O]_2\} + f\{Rh[P(O)_2N]_2\} \cdot r\{Rh[P(O)_2N]_2\} \cdot S_R\{Rh[P(O)_2N]_2\} + f\{Rh[P(O)_2O][P(O)_2N]\} \cdot r\{Rh[P(O)_2O][P(O)_2N]\} \cdot S_R\{Rh[P(O)_2O][P(O)_2N]\}$$

$$E(S) = f\{Rh[P(O)_2O]_2\} \cdot r\{Rh[P(O)_2O]_2\} \cdot S_S\{Rh[P(O)_2O]_2\} + f\{Rh[P(O)_2N]_2\} \cdot r\{Rh[P(O)_2N]_2\} \cdot S_S\{Rh[P(O)_2N]_2\} + f\{Rh[P(O)_2O][P(O)_2N]\} \cdot r\{Rh[P(O)_2O][P(O)_2N]\} \cdot S_S\{Rh[P(O)_2O][P(O)_2N]\}$$

where E is the amount of enantiomer, f the fraction of a catalytic species, r the relative rate and S the enantioselectivity. The fractions of each complex, f $Rh[P(O)_2O]_2$, f $Rh[P(O)_2N]_2$, and f $Rh[P(O)_2O][P(O)_2N]$ depend on the amount of $P(O)_2O$ and $P(O)_2N$ used {which is equal to 2-$P(O)_2O$}, and on the equilibrium constant (*K*) as already shown in Figure 13.

Before trying to fit the model to the experimental data, we investigated what, according to our model, the effects of both the equilibrium constant (*K*) and the rate ratios would be on the overall variation of the *ee* with the $P(O)_2O/P(O)_2N$ ratio.

Effect of *K*, the equilibrium constant between the different catalytic species: In Figure 14, a set of curves representing the variation of the *ee* with the amount of $P(O)_2O$ for different values of *K* are plotted. These curves were obtained with the following parameters for the individual catalytic species: $Rh[P(O)_2O]_2$: r = 20, *ee* = 25%, $Rh[P(O)_2N]_2$:

r = 1, *ee* = 25%, $Rh[P(O)_2O][P(O)_2N]$: r = 10, *ee* = 95%, that is, based on the experimental observations where $Rh[P(O)_2O]_2$ appears to be much faster than $Rh[P(O)_2N]_2$, and the hetero-complex is more enantioselective than both homo-complexes.

The first comment we can make is that the obtained curves match grossly the one obtained experimentally. They indeed show improved *ee* for the mixture of ligands. As can be seen upon examination of Figure 14, the optimal catalytic mixture (i.e., the mixture giving the highest *ee*) is obtained for an excess of $P(O)_2N$ [low $P(O)_2O$ amount] when *K* is low. When *K* increases, the optimal ratio $P(O)_2O$ to $P(O)_2N$ increases and becomes close to 1:1 for $K=500$. Moreover, for this large value of *K*, the curve is more flat at its optimum. This can be easily interpreted. For low *K* values, the concentration of the homo-complexes is important and one needs to use a large excess of $P(O)_2N$ ligand to reduce significantly the amount of the fast but not selective $Rh[P(O)_2O]_2$ catalyst. On the contrary, for high *K* values the main catalytic species is always the hetero-complex and consequently decreasing the amount of $P(O)_2O$ does not lead to a significant improvement.

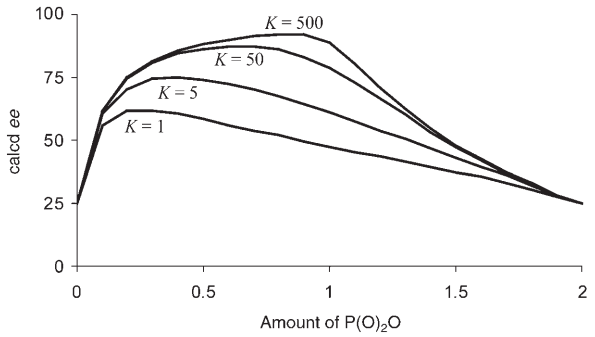

Figure 14. Effect of *K* on the variation of the *ee* with the $P(O)_2O/P(O)_2N$ ratio ($P(O)_2O+P(O)_2N$/Rh 2:1) {$Rh[P(O)_2O]_2$: r = 20, *ee* 25%; $Rh[P(O)_2N]_2$: r = 1, *ee* 25%; $Rh[P(O)_2O][P(O)_2N]$: r = 10, *ee* 95%}.

Effect of the relative rate of the hetero-complex: As already mentioned, it was observed experimentally that the $Rh[P(O)_2O]_2$ catalyst is much faster than the $Rh[P(O)_2N]_2$. An intermediate rate between the ones of the $Rh[P(O)_2O]_2$ and $Rh[P(O)_2N]_2$ species was attributed to the $Rh[P(O)_2O][P(O)_2N]$ catalyst, based on the fact that the overall rate measured in the case of the mixture of ligands is intermediate between the ones of the two pure homo-complexes. However, the precise relative rate of the $Rh[P(O)_2O][P(O)_2N]$ catalyst cannot be determined and consequently, is the second variable (with *K*) of our model. At this stage, we examined how it influences the shape of our calculated curves (*ee* vs $P(O)_2O/P(O)_2N$ ratio). For this purpose, we assigned the following values to the individual catalytic species: $Rh[P(O)_2O]_2$: r = 50, *ee* = 25%; $Rh[P(O)_2N]_2$: r = 1, *ee* = 25%; $Rh[P(O)_2O][P(O)_2N]$: r varies, *ee* = 95%, and *K* was set to 5. The calculated curves for various values of the relative rate of the $Rh[P(O)_2O][P(O)_2N]$ species are shown in Figure 15.

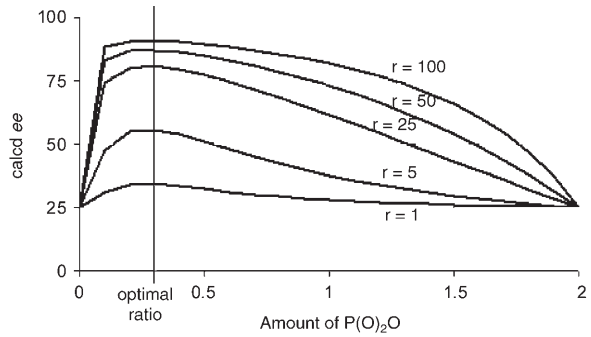

Figure 15. Effect of the rate of the $Rh[P(O)_2O][P(O)_2N]$ species on the variation of the *ee* with $P(O)_2O/P(O)_2N$ ratio [$P(O)_2O+P(O)_2N$/Rh 2:1] {$Rh[P(O)_2O]_2$: r = 50, *ee* 25%; $Rh[P(O)_2N]_2$: r = 1, *ee* 25%; $Rh[P(O)_2O][P(O)_2N]$: *ee* 95%, $K=5$}.

As can be seen in Figure 15, varying the rate of the pure $Rh[P(O)_2O][P(O)_2N]$ catalyst does not change the position of the optimal ratio $P(O)_2O/P(O)_2N$ [$P(O)_2O$ = 0.25/$P(O)_2N$ = 1.75]. Nevertheless, it has an important effect over the best value obtained for the *ee* {from 34% for r $Rh[P(O)_2O][P(O)_2N]$ = 1 to 90% for r $Rh[P(O)_2O][P(O)_2N]$ = 100}. Moreover, the shape of the curve in the excess $P(O)_2O$ region changes a lot with the value of r $Rh[P(O)_2O][P(O)_2N]$ from concave to convex. This can also be explained quite simply by considering that the effect of a slow $Rh[P(O)_2O][P(O)_2N]$ catalyst will be observed only when the relative amount of the fast $Rh[P(O)_2O]_2$ will be low, that is, at low $P(O)_2O$ amounts. On the contrary, if the $Rh[P(O)_2O][P(O)_2N]$ species is faster than the $Rh[P(O)_2O]_2$ species, it will make a significant contribution to the observed *ee* even at high $P(O)_2O$ levels, rendering the curve convex.

Two conclusions can be drawn from our simple model:

- The optimal ligand ratio is entirely dependent on the equilibrium constant (*K*) between the two homo-complexes and the hetero-complex. This means that for each combination of $P(O)_2O/P(O)_2N$ ligands, there is an optimal ratio $P(O)_2O/P(O)_2N$, eventually different from the 1:1 mixture, leading to the highest *ee*.
- The position of the optimal ratio $P(O)_2O/P(O)_2N$ does not depend on the intrinsic activity of each of the three hypothetic catalytic species. Nevertheless, if the hetero-complex has an intrinsic activity much lower than the unselective fast homo-complex, a sharper maximum is to be expected in the (*ee* vs ligand ratio) curves.

Fitting the model to the experimental data: By varying the three handles of our model, that is, the equilibrium constant (*K*) of the three catalytic species, the relative rate of the hetero-complex, r $Rh[P(O)_2O][P(O)_2N]$, and within a

certain extent the *ee* of the hetero-complex Rh[P(O)$_2$O]-[P(O)$_2$N] (assumed to be at least equal or better than the best obtained *ee* for the ligand mixture), we tried to fit the model to the experimental data.

1) **6**-P(O)$_2$O/**12**-P(O)$_2$N—Hydrogenation of methyl 2-acetamidocinnamate (*i*PrOH).
   For this ligands system, a good fit between the model and the experiment (see Figure 16) is obtained with the following values for the different complexes:

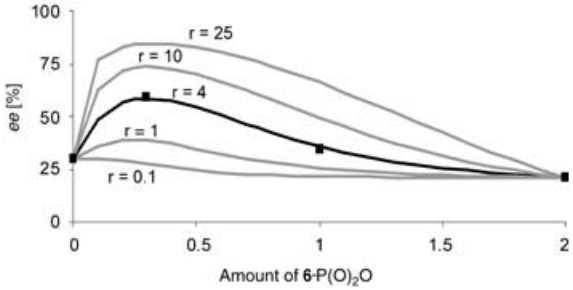

Figure 16. Experimental (■) and calculated (——) *ee* values vs **6**-P(O)$_2$O/**12**-P(O)$_2$N ratio for different values of r {Rh[**12**-P(O)$_2$N][**6**-P(O)$_2$O]}; experimental data obtained with [Rh(cod)$_2$BF$_4$] (0.01 mmol), methyl 2-acetamidocinnamate (0.2 mmol), *i*PrOH (5 mL), H_2 (5 bar), room temperature, 6 h.

   $K = 10$
   relative rates:
   r {Rh[**6**-P(O)$_2$O]$_2$} = 50
   r {Rh[**12**-P(O)$_2$N][**6**-P(O)$_2$O]} = 4
   r {Rh[**12**-P(O)$_2$N]$_2$} = 1
   selectivity:
   ee {Rh[**6**-P(O)$_2$O]$_2$} = 21
   ee {Rh[**12**-P(O)$_2$N]$_2$} = 30
   ee {Rh[**12**-P(O)$_2$N][**6**-P(O)$_2$O]} = 95
   It is worth noting that the best fit is obtained assuming that *K* is higher than 1, that is, that there is a preference for the hetero-complex over the homo-complexes. Moreover, the hetero-complex is still slow compared to the Rh[**6**-P(O)$_2$O]$_2$ homo-complex (around 10 times) and consequently must be highly selective.
2) **4**-P(O)$_2$O/**13**-P(O)$_2$N—Hydrogenation of methyl 2-acetamidocinnamate (*i*PrOH).
   For this ligands system, the best fit is obtained with the following values for the different complexes (Figure 17):
   $K = 250$
   relative rates:
   r {Rh[**4**-P(O)$_2$O]$_2$} = 50
   r {Rh[**13**-P(O)$_2$N][**4**-P(O)$_2$O]} = 15
   r {Rh[**13**-P(O)$_2$N]$_2$} = 0.1
   selectivity:
   ee {Rh[**4**-P(O)$_2$O]$_2$} = 79
   ee {Rh[**13**-P(O)$_2$N]$_2$} = 36
   ee {Rh[**13**-P(O)$_2$N][**4**-P(O)$_2$O]} = 99
   In this case, the model predicts a higher value of *K* than for the preceding case. Moreover, the rate difference between the fast homo-complex Rh[**4**-P(O)$_2$O]$_2$ and the hetero-complex is only a factor 3 while the slow homo-complex Rh[**13**-P(O)$_2$N]$_2$ is now two orders of magnitude slower compared to both other species.

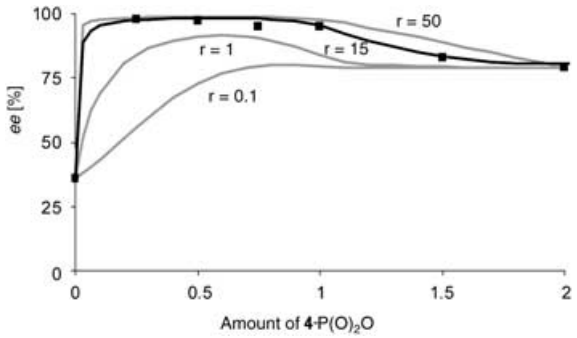

Figure 17. Experimental (■) and calculated (——) *ee* values vs **4**-P(O)$_2$O/**13**-P(O)$_2$N ratio for different values of r {Rh[**13**-P(O)$_2$N][**4**-P(O)$_2$O]}; experimental data obtained with [Rh(cod)$_2$BF$_4$] (0.01 mmol), methyl 2-acetamidocinnamate (0.2 mmol), *i*PrOH (5 mL), H_2 (5 bar), room temperature, 6 h.

3) **3**-P(O)$_2$O/**19**-P(O)$_2$N—Hydrogenation of methyl (*Z*)-3-acetamidocrotonate (*i*PrOH).
   For this ligands system, the Rh[**19**-P(O)$_2$N]$_2$ homo-complex has been shown to be as active as Rh[**3**-P(O)$_2$O]$_2$ homo-complex. This fits well with the model where the best fit is obtained with the following values (Figure 18).
   $K = 25$
   relative rates:
   r {Rh[**3**-P(O)$_2$O]$_2$} = 55
   r {Rh[**19**-P(O)$_2$N[][**3**-P(O)$_2$O]} = 30
   r {Rh[**19**-P(O)$_2$N]$_2$} = 30
   selectivity:
   ee {Rh[**3**-P(O)$_2$O]$_2$} = 19
   ee {Rh[**19**-P(O)$_2$N]$_2$} = 22
   ee {Rh[**19**-P(O)$_2$N][**3**-P(O)$_2$O]} = 95
   In this model, one can notice that the rate of the three Rh complexes are in the same order of magnitude and that *K* has an average value to permit some contribution of the homo-complexes in the 1:1 **3**-P(O)$_2$O/**19**-P(O)$_2$N ratio region.

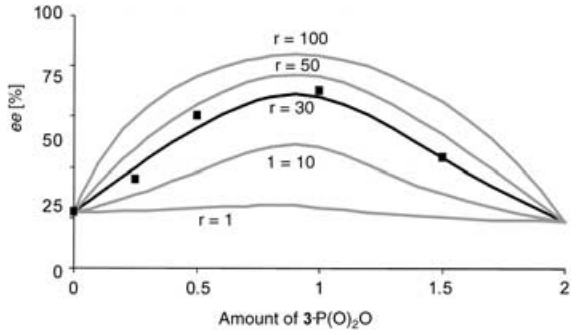

Figure 18. Experimental (■) and calculated (——) *ee* values vs **3**-P(O)$_2$O/**19**-P(O)$_2$N ratio for different values of r {Rh[**19**-P(O)$_2$N][**3**-P(O)$_2$O]}; experimental data obtained with [Rh(cod)$_2$BF$_4$] (0.01 mmol), methyl (*Z*)-3-acetamidocrotonate (0.2 mmol), *i*PrOH (5 mL), H_2 (25 bar), room temperature, 6 h.

In summary, we built a model for the description of the behaviors observed when non-equivalent amount of the two ligands are used. As simple as it is, this model can be used to fit the experimental data and consequently provides semi-quantitative information on values that are not accessible via the experience, such as the rate of the hetero-complexes relative to the rate of the homo-complexes. It also allows an estimation of the distribution of the homo/hetero-complexes. The model also gives guidelines whether it is pertinent to screen outside the ratio of 1:1 for the ligands and how much improvement could be expected by doing so. In general, we would recommend to use non-equivalent amounts of ligands every time the following conditions are met: i) the hetero-complex is much more enantioselective than the two corresponding homo-complexes; ii) the rates of the two homo-complexes are significantly different; iii) the equilibrium constant (K) is relatively low.

Conclusion

In conclusion, a library of 19 chiral tropos phosphorus ligands (11 phosphites and 8 phosphoramidites), based on a chiral P-bound alcohol or secondary amine and a flexible (tropos) P-bound biphenol unit, was synthesized. These ligands exist, in principle, as a mixture of two rapidly interconverting diastereomers, L^a and $L^{a'}$, differing in the conformation of the biphenol unit. Upon complexation with Rh, the ligand (L^a in equilibrium with $L^{a'}$) should give rise to three different species, namely RhL^aL^a, $RhL^aL^{a'}$, $RhL^{a'}L^{a'}$. Our novel approach consists in the use of a combination of two of these ligands (L^a in equilibrium with $L^{a'}$ and L^b in equilibrium with $L^{b'}$) resulting in the generation of a dynamic "in situ" library, with several different species (up to ten, in principle) present in solution. These ligands were screened, individually and as a combination of two, in the rhodium-catalyzed asymmetric hydrogenation of several prochiral olefins, such as dehydro-α-amino acids, dehydro-β-amino acids, enamides and unsaturated esters. *ee* values up to 98% were obtained for the dehydro-α-amino acids, by using the best combination of ligands, a phosphite, [**4**-$P(O)_2O$], and a phosphoramidite, [**13**-$P(O)_2N$]. Kinetic studies of the reactions with the single ligands and with the combination of phosphite [**4**-$P(O)_2O$] and phosphoramidite [**13**-$P(O)_2N$] were then performed, by measuring the rate of hydrogen uptake. It was shown that the phosphite, despite being less enantioselective, promotes the hydrogenation of methyl 2-acetamidoacrylate and methyl 2-acetamidocinnamate faster than the mixture of the same phosphite with the phosphoramidite, while the phosphoramidite alone is much less active. In this way, the reaction was optimized by lowering the phosphite/phosphoramidite ratio (the best ratio is 0.25 equiv phosphite/1.75 equiv phosphoramidite) with a resulting improvement of the product enantiomeric excess. A simple mathematical model for a better understanding of the variation of the enantiomeric excess with the phosphite/phosphoramidite ratio is also presented. The new concept of using a non-equivalent amount of the two ligands (while keeping total L/Rh = 2) is a novel powerful tool to enhance enantioselectivity in selected cases.

Work is in progress in our laboratories to expand the scope of this ligand-combination approach to other enantioselective transformations.

Experimental Section

General remarks: All reactions were carried out in flame-dried glassware with magnetic stirring under argon atmosphere. All commercially available reagents were used as received. The solvents were dried by distillation over the following drying agents and were transferred under nitrogen: CH_2Cl_2 (CaH_2), THF (Na), Et_2O (Na), toluene (Na), Et_3N (CaH_2), pyridine (CaH_2). Reactions were monitored by analytical thin-layer chromatography (TLC) by using silica gel 60 F_{254} precoated glass plates (0.25 mm thickness). Visualization was accomplished by irradiation with a UV lamp and/or staining with a ceric ammonium molybdate (CAM) solution. Flash column chromatography was performed by using silica gel 60 Å, particle size 40–64 μm, following the procedure by Still and coworkers.[32] Proton NMR spectra were recorded on a spectrometer operating at 400.13 MHz. Proton chemical shifts are reported in ppm (δ) with the solvent reference relative to tetramethylsilane (TMS) employed as the internal standard ($CDCl_3$ δ 7.26 ppm; [D_6]benzene, δ 7.15 ppm). The following abbreviations are used to describe spin multiplicity: s = singlet, d = doublet, t = triplet, q = quartet, m = multiplet, br = broad signal, dd = doublet of doublet. Carbon NMR spectra were recorded on a 400 spectrometer operating at 100.56 MHz, with complete proton decoupling. Carbon chemical shifts are reported in ppm (δ) relative to TMS with the respective solvent resonance as the internal standard ($CDCl_3$, δ 77.0 ppm). ^{31}P NMR spectra were recorded on a 400 spectrometer operating at 162 MHz, with complete proton decoupling. ^{31}P NMR chemical shifts are reported in ppm (δ) relative to external 85% H_3PO_4 at 0 ppm (positive values downfield). Infrared spectra were recorded on a standard FT/IR; peaks are reported in cm^{-1}. Optical rotation values were measured on an automatic polarimeter with a 1 dm cell at the sodium D line. Gas chromatography was performed on a GC instrument equipped with a flame ionization detector, by using a chiral capillary column. HPLC analyses were performed with a chiral stationary phase column. High resolution mass spectra (HRMS) were performed on a hybrid quadrupole time of flight mass spectrometer equipped with an ESI ion source. A Reserpine solution 100 $pg\,\mu L^{-1}$ (about 100 $counts^{-1}$), 0.1% HCOOH/CH_3CN 1:1, was used as reference compound (Lock Mass).

General procedure for the synthesis of phosphites (Method A): PCl_3 (2 equiv, 6 mmol, 525 μL) was added to a solution of the alcohol (1 equiv, 3 mmol) in dichloromethane (17 mL), in a Schlenk tube, under argon, at room temperature. After stirring for 2 h, the solvent and excess PCl_3 were removed under reduced pressure. The resulting residue was dissolved in tetrahydrofuran (7 mL), and a solution of the biphenol (1 equiv, 3 mmol) and triethylamine (3 equiv, 9 mmol, 1.25 mL) in THF (10 mL) was slowly added. Upon addition, the formation of a white precipitate was observed immediately. The reaction mixture was left under stirring overnight, before being filtered over a PTFE membrane filter. The solvent was removed and the crude product was purified either by recrystallisation, or by chromatography, to give the desired compound as a white foamy solid.

Several phosphites reported in Figure 2 [**2**-$P(O)_2O$, **3**-$P(O)_2O$, **5**-$P(O)_2O$, **7**-$P(O)_2O$, **8**-$P(O)_2O$, **9**-$P(O)_2O$] had previously been synthesized by Xiao and Chen.[29] However, their results were influenced by experimental problems associated with the purity of the ligands. In fact, in our hands this class of compounds shows a single set of signals at room temperature by ^1H, ^{13}C and ^{31}P NMR (see below), confirming their tropos nature. Only upon complexation with Rh, two sets of signals might possibly be observed at low temperature (−65 °C).[33] This is in sharp contrast to the information from the Xiao and Chen paper, where the ligands were de-

scribed to display two singlets (^{31}P NMR) with the same intensity (1:1 ratio) at room temperature (without Rh).[29]

General procedure for the synthesis of phosphoramidites (Method B): A solution of the amine (1 equiv, 3 mmol) and triethylamine (1.13 equiv, 3.4 mmol, 472.5 μL) in dry toluene (2.6 mL) was added to a solution of PCl_3 (1 equiv, 3 mmol, 262 μL) in toluene (38 mL), in a Schlenk tube, under argon. The reaction mixture was heated to 70 °C for 6 h, and allowed to cool to room temperature. Triethylamine (2.26 equiv, 6.78 mmol, 945 μL) was added, and the mixture was cooled to −78 °C. A solution of biphenol (1 equiv, 3 mmol) in toluene/THF 4:1 (7.5 mL) was added slowly. The reaction mixture was left under stirring overnight, allowing to slowly warm to room temperature. The mixture was filtered over a pad of Celite, and the solvent removed under reduced pressure. The crude product was purified either by recrystallisation, or by chromatography, to give the desired compound as a white powder.

Bis-[(*S*)-1-naphth-1-yl-ethyl]amine and bis-[(*R*)-1-naphth-1-yl-ethyl]-amine were synthesized in two steps, as reported in literature.[34] (*R*,*R*)-2,5-diphenylpyrrolidine and (*S*,*S*)-2,5-diphenylpyrrolidine were prepared following literature procedure.[35] 3,3′,5,5′-Tetramethyl-biphenol[14d] and 3,3′,5,5′-tetra-*tert*-butyl-biphenol[36] were prepared following the reported procedures.

1-P(O)$_2$O, **biphenol/(1*S*,2*R*,5*S*)-(+)-menthol**: 97 % yield; $[\alpha]_D = +17.4$ ($c = 1.00$ in chloroform).

2-P(O)$_2$O, biphenol/(1*R*,2*S*,5*R*)-(−)-menthol: 88 % yield; m.p. 98 °C; $[\alpha]_D = -17.4$ (c = 1.00 in chloroform); ^{1}H NMR (400 MHz, $CDCl_3$, 25 °C): $\delta = 7.49$ (d, ^3J(H,H) = 7.6 Hz, 2H, ArH), 7.37 (t, ^3J(H,H) = 7.6 Hz, 2H, ArH), 7.30 (t, ^3J(H,H) = 7.5 Hz, 2H, ArH), 7.22–7.20 (m, 2H, ArH), 4.20–4.16 (m, 1H, CH), 2.32–2.27 (m, 1H, CH), 2.25–2.18 (m, 1H, CH), 1.73–1.69 (m, 2H, CH), 1.51–1.35 (m, 2H, CH), 1.08–1.04 (m, 3H, CH), 0.99 (d, ^3J(H,H) = 6.5 Hz, 3H, CH_3), 0.96 (d, ^3J(H,H) = 7.0 Hz, 3H, CH_3), 0.88 ppm (d, ^3J(H,H) = 6.9 Hz, 3H, CH_3); ^{13}C NMR (100 MHz, $CDCl_3$, 25 °C): $\delta = 156.0$, 149.8, 131.8, 130.3, 129.4, 128.1, 125.4, 122.5, 120.3, 118.5, 76.7 (d, J(C,P) = 17.4 Hz), 48.9, 44.6, 34.5, 32.2, 25.7, 23.3, 22.5, 21.4, 16.0 ppm; ^{31}P NMR (162 MHz, $CDCl_3$, 25 °C): $\delta = 152.8$ ppm; IR (CCl_4): $\tilde{\nu}_{max} = 3068$, 3030, 2958, 2871, 1943, 1910, 1600, 1570, 1556, 1545, 1499, 1476, 1438, 1386, 1370, 1271, 1249, 1210, 1187, 1097, 1013, 992, 900 cm^{-1}; HRMS (ESI): m/z: calcd for $[C_{22}H_{27}NaO_3P]^+$: 393.1595; found: 393.1579 $[M+Na]^+$; elemental analysis calcd for $C_{22}H_{27}O_3P$: C 71.33, H 7.35; found: C 71.23, H 7.32.

3-P(O)$_2$O, **biphenol/(1*R*,2*R*,3*R*,5*S*)-(−)-isopinocampheol**: 76 % yield; m.p. 106 °C; $[\alpha]_D = -17.0$ ($c = 1.00$ in chloroform); ^{1}H NMR (400 MHz, $CDCl_3$, 25 °C): $\delta = 7.49$ (d, ^3J(H,H) = 7.6 Hz, 2H, ArH), 7.38 (t, ^3J(H,H) = 7.6 Hz, 2H, ArH), 7.29 (t, ^3J(H,H) = 7.6 Hz, 2H, ArH), 7.21 (t, ^3J(H,H) = 7.6 Hz, 2H, ArH), 4.77–4.69 (m, 1H, CH), 2.59–2.52 (m, 1H, CH), 2.41–2.36 (m, 1H, CH), 2.27–2.23 (m, 1H, CH), 2.10–2.03 (m, 1H, CH), 1.99–1.97 (m, 1H, CH), 1.87–1.84 (m, 1H, CH), 1.25 (s, 3H, CH_3), 1.20 (d, ^3J(H,H) = 7.2 Hz, 3H, CH_3), 1.15 (d, ^3J(H,H) = 10 Hz, 1H, CH), 0.91 ppm (s, 3H, CH_3); ^{13}C NMR (100 MHz, $CDCl_3$, 25 °C): $\delta = 150.0$, 130.4, 129.4, 125.4, 122.6, 122.4, 76.1 (d, J(C,P) = 15 Hz), 48.2, 46.1, 42.0, 38.8, 38.2, 34.4, 28.0, 24.3, 20.4 ppm; ^{31}P NMR (162 MHz, $CDCl_3$, 25 °C): $\delta =$ 147.7 ppm; IR (CCl_4): $\tilde{\nu}_{max} = 3069$, 3029, 2959, 2910, 2872, 1943, 1911, 1601, 1567, 1553, 1499, 1476, 1437, 1386, 1370, 1260, 1249, 1210, 1187, 1097, 996, 942, 897, 857 cm^{-1}; HRMS (ESI): m/z: calcd for $[C_{22}H_{27}NaO_4P]^+$: 409.1545; found: 409.1538 $[M+Na+H_2O]^+$; elemental analysis calcd for $C_{22}H_{25}O_3P$: C 71.72, H 6.84; found: C 71.80, H 6.86.

4-P(O)$_2$O, biphenol/(1*R*,2*S*)-(−)-*trans*-2-phenyl-1-cyclohexanol: 63 % yield; m.p. 117 °C; $[\alpha]_D = -53.6$ ($c = 1.00$ in chloroform); ^{1}H NMR (400 MHz, [D$_6$]benzene, 25 °C): $\delta = 7.46$–6.90 (m, 12H, ArH), 6.50–6.40 (m, 1H, ArH), 4.50–4.38 (m, 1H, CyH), 2.80–2.65 (m, 1H, CyH), 2.35–2.20 (m, 1H, CyH), 2.10–1.20 ppm (m, 7H, CyH); ^{13}C NMR (100 MHz, [D$_6$]benzene, 25 °C): $\delta = 149.9$, 143.9, 130.4, 130.1, 129.5, 129.4, 129.1, 129.0, 128.4, 127.3, 125.5, 125.4, 122.8, 122.7, 79.3 (d, J(C,P) = 17 Hz), 52.2, 36.0, 34.5, 26.3, 25.7 ppm; ^{31}P NMR (162 MHz, [D$_6$]benzene, 25 °C): $\delta = 151.5$ ppm; IR (CCl_4): $\tilde{\nu}_{max} = 3066$, 3031, 2961, 2936, 2859, 1942, 1911, 1604, 1556, 1498, 1476, 1437, 1260, 1250, 1210, 1187, 1097, 1025, 901, 855, 831 cm^{-1}; HRMS (ESI): m/z: calcd for $[C_{24}H_{25}NaO_4P]^+$: 431.1388; found: 431.1370 $[M+Na+H_2O]^+$; elemental analysis calcd for $C_{24}H_{23}O_3P$: C 73.83, H 5.94; found: C 71.15, H 6.16.

5-P(O)$_2$O, **biphenol/(−)-borneol**: 82 % yield; m.p. 88 °C; $[\alpha]_D = -5.5$ ($c =$ 1.00 in chloroform); ^{1}H NMR (400 MHz, $CDCl_3$, 25 °C): $\delta = 7.49$ (d, ^3J (H,H) = 7.6 Hz, 2H, ArH), 7.40–7.36 (m, 2H, ArH), 7.30–7.26 (m, 2H, ArH), 7.20 (d, ^3J(H,H) = 8.0 Hz, 2H, ArH), 4.62–4.56 (m, 1H, CH), 2.26–2.18 (m, 1H, CH), 2.06–2.00 (m, 1H, CH), 1.87–1.62 (m, 2H, CH), 1.32–1.24 (m, 3H, CH), 0.94 (s, 3H, CH_3), 0.88 (s, 3H, CH_3), 0.77 ppm (s, 3H, CH_3); ^{13}C NMR (100 MHz, $CDCl_3$, 25 °C): $\delta = 150.2$, 131.6, 131.5, 130.3, 129.4, 129.3, 125.3, 122.5, 81.5, 50.2, 48.1, 45.4, 38.4, 28.5, 26.9, 20.4, 19.0, 13.8 ppm; ^{31}P NMR (162 MHz, $CDCl_3$, 25 °C): $\delta = 145.4$ ppm; IR (CCl_4): $\tilde{\nu}_{max} = 3069$, 3030, 2961, 2881, 2453, 1943, 1601, 1499, 1476, 1438, 1264, 1210, 1188, 1097, 891, 858 cm^{-1}; HRMS (ESI): m/z: calcd for $[C_{22}H_{25}NaO_3P]^+$: 391.1439; found: 391.1427 $[M+Na]^+$; elemental analysis calcd for $C_{22}H_{25}O_3P$: C 71.72, H 6.84; found: C 71.78, H 6.87.

6-P(O)$_2$O, **biphenol/(1*R*,2*S*)-(−)-*trans*-(1-methyl-1-phenylethyl)cyclohexanol**: 79 % yield; m.p. 128 °C; $[\alpha]_D = -12.6$ ($c = 1.00$ in chloroform); ^{1}H NMR (400 MHz, $CDCl_3$, 25 °C): $\delta = 7.58$–7.10 (m, 13H, ArH), 4.32–4.24 (m, 1H, CH), 2.28–2.24 (m, 1H, CH), 1.99–1.92 (m, 1H, CH), 1.76–1.56 (m, 3H, CH), 1.50 (s, 3H, CH_3), 1.46 (s, 3H, CH_3), 1.38–1.19 (m, 1H, CH); 1.19–0.88 ppm (m, 3H, CH); ^{13}C NMR (100 MHz, $CDCl_3$, 25 °C): $\delta = 150.3$, 149.6, 131.4, 129.9, 129.4, 129.0, 127.9, 126.0, 125.3, 124.9, 124.8, 122.2, 122.0, 121.0, 117.0, 77.5 (d, J(C,P) = 16 Hz), 52.6, 40.8, 36.8, 30.4, 27.6, 25.6, 24.8, 24.6 ppm; ^{31}P NMR (162 MHz, $CDCl_3$, 25 °C): $\delta = 153.4$ ppm; IR (CCl_4): $\tilde{\nu}_{max} = 3065$, 3031, 2935, 2859, 1943, 1553, 1499, 1476, 1437, 1260, 1210, 1187, 1098, 1016, 900, 847, 830 cm^{-1}; HRMS (ESI): m/z: calcd for $[C_{27}H_{29}NaO_3P]^+$: 455.1752; found: 455.1743 $[M+Na]^+$; elemental analysis calcd for $C_{27}H_{29}O_3P$: C 74.98, H 6.76; found: C 72.39, H 6.90.

7-P(O)$_2$O, **3,3′,5,5′-tetra-*tert*-butylbiphenol/(1*R*,2*R*,3*R*,5*S*)-(−)-isopinocampheol**: 87 % yield; m.p. 75 °C; $[\alpha]_D = +5.3$ ($c = 1.00$ in chloroform); ^{1}H NMR (400 MHz, $CDCl_3$, 25 °C): $\delta = 7.53$–7.51 (m, 1H, ArH), 7.45–7.43 (m, 1H, ArH), 7.28–7.26 (m, 1H, ArH), 7.19–7.17 (m, 1H, ArH), 4.75–4.57 (m, 1H, CH), 2.59–2.52 (m, 1H, CH), 2.41–2.36 (m, 1H, CH), 2.27–2.23 (m, 1H, CH), 2.10–1.94 (m, 2H, CH), 1.87–1.84 (m, 1H, CH), 1.50 (s, 18H, *t*Bu), 1.45 (s, 3H, CH_3), 1.36 (s, 18H, *t*Bu), 1.20 (d, ^3J (H,H) = 7.2 Hz, 3H, CH_3), 1.06 (d, ^3J(H,H) = 10 Hz, 1H, CH), 0.89 ppm (s, 3H, CH_3); ^{13}C NMR (100 MHz, $CDCl_3$, 25 °C): $\delta = 127.0$, 126.9, 125.4, 124.5, 76.7, 48.2, 46.0, 45.7, 42.0, 38.2, 33.9, 31.9, 31.8, 31.6, 27.9, 24.3, 20.5 ppm; ^{31}P NMR (162 MHz, $CDCl_3$, 25 °C): $\delta = 146.7$ ppm; IR (CCl_4): $\tilde{\nu}_{max} = 2963$, 2907, 2871, 2448, 1945, 1595, 1556, 1545, 1475, 1440, 1397, 1363, 1260, 1229, 1094, 1018, 937, 879 cm^{-1}; HRMS (ESI): m/z: calcd for $[C_{38}H_{57}NaO_3P]^+$: 615.3943; found: 615.3935 $[M+Na]^+$; elemental analysis calcd for $C_{38}H_{57}O_3P$: C 76.99, H 9.69; found: C 77.02, H 9.71.

8-P(O)$_2$O, **3,3′,5,5′-tetra-*tert*-butylbiphenol/(1*R*,2*S*,5*R*)-(−)-menthol**: 84 % yield; m.p. 140 °C; $[\alpha]_D = -17.3$ ($c = 1.00$ in chloroform); ^{1}H NMR (400 MHz, $CDCl_3$, 25 °C): $\delta = 7.44$ (s, 1H, ArH), 7.43 (s, 1H, ArH), 7.19 (s, 1H, ArH), 7.18 (s, 1H, ArH), 4.11–4.06 (m, 1H, CH), 2.25–2.15 (m, 1H, CH), 2.10–1.80 (m, 2H, CH), 1.70–1.55 (m, 2H, CH), 1.50 (s, 18H, 2 × *t*Bu), 1.50–0.60 (m, 4H, CH), 1.36 (s, 18H, 2 × *t*Bu), 0.87–0.84 (m, 6H, 2 × CH_3), 0.73 ppm (d, ^3J(H,H) = 6.9 Hz, 3H, CH_3); ^{13}C NMR (100 MHz, $CDCl_3$, 25 °C): $\delta = 150.0$, 131.7, 130.3, 129.4, 125.4, 122.5, 79.1, 76.7, 76.6, 58.3, 48.9, 44.5, 34.5, 32.2, 25.7, 23.3, 22.5, 21.4, 16.0 ppm; ^{31}P NMR (162 MHz, $CDCl_3$, 25 °C): $\delta = 147.0$ ppm; IR (CCl_4): $\tilde{\nu}_{max} = 2962$, 2870, 1595, 1558, 1547, 1456, 1413, 1396, 1362, 1093, 1017 cm^{-1}; HRMS (ESI): m/z: calcd for $[C_{38}H_{59}NaO_3P]^+$: 617.4099; found: 617.4093 $[M+Na]^+$; elemental analysis calcd for $C_{38}H_{59}O_3P$: C 76.73, H 10.00; found: C 76.69, H 9.97.

9-P(O)$_2$O, **biphenol/(1*R*)-*endo*-(+)-fenchol**: 78 % yield; m.p. 104 °C; $[\alpha]_D = +9.8$ ($c = 1.00$ in chloroform); ^{1}H NMR (400 MHz, $CDCl_3$, 25 °C): $\delta = 7.50$ (d, ^3J(H,H) = 7.6 Hz, 2H, ArH), 7.44–7.21 (m, 6H, ArH), 3.96 (d, ^3J(H,H) = 11.6 Hz, 1H, CH), 1.85–1.67 (m, 4H, CH), 1.58–1.40 (m, 3H, CH), 1.24 (s, 3H, CH_3), 1.04 (s, 3H, CH_3), 0.96 ppm (s, 3H, CH_3); ^{13}C NMR (100 MHz, $CDCl_3$, 25 °C): $\delta = 130.5$, 129.6, 125.6, 125.5, 122.9, 89.2 (d, J(C,P) = 12.0 Hz), 50.1, 48.8, 41.8, 40.4, 30.6, 26.7, 26.5, 22.2, 20.2 ppm; ^{31}P NMR (162 MHz, $CDCl_3$, 25 °C): $\delta = 148.6$ ppm; IR (CCl_4): $\tilde{\nu}_{max} = 3069$, 3030, 2962, 2873, 1944, 1911, 1602, 1569, 1556, 1499, 1476, 1437, 1260, 1210, 1187, 1098, 1015, 904, 857 cm^{-1}; HRMS (ESI): m/z: calcd for $[C_{22}H_{25}NaO_3P]^+$: 391.1439; found: 391.1423 $[M+Na]^+$; elemental analysis calcd for $C_{22}H_{25}O_3P$: C 71.72, H 6.84; found: C 69.42, H 7.07.

10-P(O)$_2$O, **3,3′,5,5′-tetramethylbiphenol/(−)-borneol**: 76% yield; m.p. 81°C; $[\alpha]_D = +2.5$ ($c = 1.01$ in chloroform); ^{1}H NMR (400 MHz, $CDCl_3$, 25°C): $\delta = 7.13$ (s, 2H, ArH), 7.08 (s, 2H, ArH), 4.65–4.60 (m, 1H, CH), 2.40 (s, 12H, 4×CH_3), 2.27–2.20 (m, 1H, CH), 2.07–2.00 (m, 1H, CH), 1.76–1.67 (m, 2H, CH), 1.33–1.23 (m, 3H, CH), 0.96 (s, 3H, CH_3), 0.91 (s, 3H, CH_3), 0.86 ppm (s, 3H, CH_3); ^{13}C NMR (100 MHz, $CDCl_3$, 25°C): $\delta = 134.2$, 131.6, 130.6, 128.6, 81.8 (d, J(C,P) = 12.0 Hz), 50.5, 48.4, 45.7, 38.5, 28.9, 27.3, 21.6, 20.8, 19.4, 17.5, 14.1 ppm; ^{31}P NMR (162 MHz, $CDCl_3$, 25°C): $\delta = 145.7$ ppm; IR (CCl_4): $\tilde{\nu}_{max} = 2957$, 2880, 1557, 1478, 1260, 1245, 1214, 1188, 1154, 1119, 1030, 866, 830 cm^{-1}; HRMS (ESI): m/z: calcd for $[C_{26}H_{35}NaO_4P]^+$: 465.2171; found: 465.2141 $[M+Na+H_2O]^+$; elemental analysis calcd for $C_{26}H_{33}O_3P$: C 73.56, H 7.84; found: C 72.15, H 8.06.

11-P(O)$_2$O, **3,3′,5,5′-tetramethylbiphenol/(1*R*)-*endo*-(+)-fenchol**: 78% yield; m.p. 91°C; $[\alpha]_D = -27.5$ (c = 1.01 in chloroform); ^{1}H NMR (400 MHz, $CDCl_3$, 25°C): $\delta = 7.13$ (d, ^3J(H,H) = 7.2 Hz, 2H, ArH), 7.08 (s, 2H, ArH), 3.94 (dd, $^3J_1$(H,H) = 12.0 Hz, $^3J_2$(H,H) = 1.6 Hz, 1H, CH), 2.41 (s, 6H, 2×CH_3), 2.40 (s, 6H, 2×CH_3), 1.84–1.69 (m, 4H, CH), 1.59–1.43 (m, 3H, CH), 1.21 (s, 3H, CH_3), 1.09 (s, 3H, CH_3), 0.90 ppm (s, 3H, CH_3); ^{13}C NMR (100 MHz, $CDCl_3$, 25°C): $\delta = 146.9$, 146.4, 134.3, 132.0, 131.7, 131.5, 130.7, 128.6, 88.8 (d, J(C,P) = 15.0 Hz), 50.0, 48.7, 41.9, 40.4, 30.8, 26.9, 26.4, 22.4, 21.6, 20.1, 17.7, 17.5 ppm; ^{31}P NMR (162 MHz, $CDCl_3$, 25°C): $\delta = 149.7$ ppm; IR (CCl_4): $\tilde{\nu}_{max} = 2962$, 2872, 1945, 1557, 1478, 1260, 1214, 1187, 1154, 1098, 1012, 871, 831 cm^{-1}; HRMS (ESI): m/z: calcd for $[C_{26}H_{35}NaO_4P]^+$: 465.2171; found: 465.2153 $[M+Na+H_2O]^+$; elemental analysis calcd for $C_{26}H_{33}O_3P$: C 73.56, H 7.84; found: C 72.39, H 7.98.

12-P(O)$_2$N, **biphenol/(*R*,*R*)-bis(α-methylbenzyl)amine**: 89% yield; $[\alpha]_D = +238.0$ ($c = 1.00$ in chloroform).

13-P(O)$_2$N, **biphenol/(*S*,*S*)-bis(α-methylbenzyl)amine**: 80% yield; m.p. 105°C; $[\alpha]_D = -238.0$ ($c = 1.00$ in chloroform); ^{1}H NMR (400 MHz, $CDCl_3$, 25°C): $\delta = 7.56$–7.49 (m, 2H, ArH), 7.41–7.22 (m, 6H, ArH), 7.20–7.11 (m, 10H, ArH), 4.66–4.58 (m, 2H, 2×H-benzyl), 1.77 ppm (d, ^3J(H,H) = 7.2 Hz, 6H, 2×CH_3-benzyl); ^{13}C NMR (100 MHz, $CDCl_3$, 25°C): $\delta = 151.5$, 143.4, 131.6, 130.4, 130.2, 129.5, 129.4, 128.3, 128.2, 127.0, 125.0, 124.4, 122.9, 122.4, 53.1, 53.0, 22.7 ppm; ^{31}P NMR (162 MHz, $CDCl_3$, 25°C): $\delta = 147.6$ ppm; IR (CCl_4): $\tilde{\nu}_{max} = 3065$, 3030, 2963, 2905, 1943, 1911, 1602, 1546, 1497, 1476, 1436, 1375, 1261, 1211, 1194, 1098, 1015, 889, 830 cm^{-1}; HRMS (ESI): m/z: calcd for $[C_{28}H_{26}NNaO_2P]^+$: 462.1599; found: 462.1574 $[M+Na]^+$; elemental analysis calcd for $C_{28}H_{26}NO_2P$: C 76.52, H 5.96, N 3.19; found: C 76.60, H 5.97, N 3.21.

14-P(O)$_2$N, **biphenol/(*S*)-(−)-*N*,α-dimethylbenzylamine**: 55% yield; $[\alpha]_D = +23.0$ ($c = 1.00$ in chloroform).

15-P(O)$_2$N, **biphenol/(*R*)-(+)-*N*,α-dimethylbenzylamine**: 40% yield; m.p. 109°C; $[\alpha]_D = -23.0$ ($c = 1.00$ in chloroform); ^{1}H NMR (400 MHz, $CDCl_3$, 25°C): $\delta = 7.54$–7.09 (m, 13H, ArH), 4.92–4.84 (m, 1H, CH), 2.23 (d, ^3J(H,H) = 4.8 Hz, 3H, CH_3), 1.69 ppm (d, ^3J(H,H) = 7.2 Hz, 3H, CH_3); ^{13}C NMR (100 MHz, $CDCl_3$, 25°C): $\delta = 152.3$, 142.7, 131.6, 130.3, 129.8, 129.0, 128.0, 127.7, 125.1, 125.0, 122.6, 56.3, 55.9, 27.7, 19.2 ppm; ^{31}P NMR (162 MHz, $CDCl_3$, 25°C): $\delta = 149.6$ ppm; IR (CCl_4): $\tilde{\nu}_{max} = 3067$, 3030, 2963, 2905, 1603, 1564, 1556, 1498, 1476, 1436, 1260, 1208, 1194, 1098, 1013, 934 cm^{-1}; HRMS (ESI): m/z: calcd for $[C_{21}H_{20}NNaO_2P]^+$: 372.1129; found: 372.1112 $[M+Na]^+$; elemental analysis calcd for $C_{21}H_{20}NO_2P$: C 72.20, H 5.77, N 4.01; found: C 72.31, H 5.79, N 3.98.

16-P(O)$_2$N, **biphenol/bis-[(*S*)-1-naphth-1-yl-ethyl]amine**: 60% yield; $[\alpha]_D = +204.8$ ($c = 0.53$ in chloroform).

17-P(O)$_2$N, **biphenol/bis-[(*R*)-1-naphth-1-yl-ethyl]amine**: 71% yield; m.p. not determined due to decomposition; $[\alpha]_D = -204.8$ ($c = 0.53$ in chloroform); ^{1}H NMR (400 MHz, $CDCl_3$, 25°C): $\delta = 7.95$ (d, ^3J(H,H) = 8.0 Hz, 2H, ArH), 7.62–7.22 (m, 18H, ArH), 6.86 (t, ^3J(H,H) = 7.6 Hz, 2H, ArH), 5.61–5.53 (m, 2H, 2×CH), 1.83 ppm(d, ^3J(H,H) = 7.2 Hz, 6H, 2×CH_3); ^{13}C NMR (100 MHz, $CDCl_3$, 25°C): $\delta = 139.1$, 133.8, 131.5, 130.9, 130.8, 129.9, 129.8, 129.0, 127.6, 125.9, 125.5, 125.3, 125.2, 124.7, 123.9, 123.1, 123.0, 51.5, 51.4, 23.7, 23.6 ppm; ^{31}P NMR (162 MHz, $CDCl_3$, 25°C): $\delta = 150.1$ ppm; IR (CCl_4): $\tilde{\nu}_{max} = 3053$, 2964, 2905, 2876, 1943, 1912, 1600, 1566, 1499, 1476, 1435, 1396, 1373, 1262, 1212, 1194, 1175, 1142, 1098, 1016, 960, 891, 850 cm^{-1}; HRMS (ESI): m/z: calcd for $[C_{36}H_{30}NNaO_2P]^+$: 562.1912; found: 562.1910 $[M+Na]^+$; elemental analysis calcd for $C_{36}H_{30}NO_2P$: C 80.13, H 5.60, N 2.60; found: C 80.15, H 5.63, N 2.59.

18-P(O)$_2$N, **biphenol/(*R*,*R*)-2,5-diphenylpyrrolidine**: 67% yield; $[\alpha]_D = +111.4$ ($c = 1.03$ in chloroform).

19-P(O)-N, **biphenol/(*S*,*S*)-2,5-diphenylpyrrolidine**: 73% yield; m.p. 101°C; $[\alpha]_D = -111.4$ ($c = 1.03$ in chloroform); ^{1}H NMR (400 MHz, $CDCl_3$, 25°C): $\delta = 7.50$–6.96 (m, 18H, ArH), 5.10 (d, ^3J(H,H) = 5.6 Hz, 2H, CH), 2.51–2.38 (m, 2H, CH), 1.89–1.78 ppm (m, 2H, CH); ^{13}C NMR (100 MHz, $CDCl_3$, 25°C): $\delta = 144.1$, 130.4, 129.9, 129.6, 129.2, 128.9, 127.5, 125.0, 124.4, 122.7, 122.2, 63.4, 63.1, 34.3, 33.0 ppm; ^{31}P NMR (162 MHz, $CDCl_3$, 25°C): $\delta = 149.2$ ppm; IR (CCl_4): $\tilde{\nu}_{max} = 3065$, 3029, 2963, 2904, 1943, 1603, 1546, 1497, 1476, 1436, 1261, 1211, 1097, 1019, 829 cm^{-1}; HRMS (ESI): m/z: calcd for $[C_{28}H_{24}NNaO_2P]^+$: 460.1442; found: 460.1431 $[M+Na]^+$; elemental analysis calcd for $C_{28}H_{24}NO_2P$: C 76.87, H 5.53, N 3.20; found: C 76.70, H 6.00, N 3.21.

General procedure for the Rh-catalyzed asymmetric hydrogenations at ambient hydrogen pressure: Hydrogenation reactions were performed by using standard Schlenk techniques. Seven flame-dried glass test tubes with stirring bars were placed in a Schlenk, under argon. In each test tube, the ligands (0.02 equiv, 0.002 mmol L^a and 0.002 mmol L^b) and [Rh(cod)$_2$BF$_4$] (0.01 equiv, 0.002 mmol, 0.8 mg) were weighed and dry dichloromethane was added (1 mL). After 30 min under stirring, a solution of the substrate (0.2 mmol) in the appropriate solvent (1 mL) was added, and the reaction mixtures were purged with argon, followed by two vacuum/hydrogen cycles. The reactions were left stirring overnight at room temperature under ambient H_2 pressure. Samples were taken for chiral GC analysis.

General procedure for the Rh-catalyzed asymmetric hydrogenations at 5–25 bar hydrogen pressure in the 96-Multireactor:[25] Stock solutions of the ligands (0.0233 M) were prepared in dry dichloromethane, and stored in a glovebox. A solution of [Rh(cod)$_2$BF$_4$] in dry dichloromethane was prepared prior to use (0.0175 M); the substrate was dissolved in the appropriate solvent. In a glovebox, 0.15 mL of each of the stock solutions of ligands L^a and L^b were dispensed (using a Zinnser Lizzy robot) in the reaction vessels (96 vessels, in a 12×8 plate). 0.2 mL of the stock solution of rhodium were added, followed by addition of 2.25 mL of the solution of the substrate (0.0311 M for substrate: Rh = 20, 0.0778 M for substrate: Rh = 50). The reactions were capped, and hydrogenated at the hydrogen pressure required, overnight. After completion, the reactors were opened and samples were analysed by chiral GC for conversion and *ee* determination.

General procedure for the Rh-catalyzed asymmetric hydrogenations in the Argonaut Endeavor multireactor autoclave: The autoclave allowed eight hydrogenation reactions in parallel in glass vessels. L^a (0.01 mmol) and L^b (0.01 mmol) [or alternatively, 0.02 mmol of a single ligand], [Rh(cod)$_2$BF$_4$] (0.01 mmol, 4.06 mg) and the substrate (0.2 mmol) were weighed in the reaction vessels. The vessels were placed in the reactor and the appropriate solvent was added (5 mL). The reaction vessels were then semi-automatically purged repeatedly with N_2 and H_2, before applying a hydrogen pressure and stirring. After completion of the reaction, the reactors were opened and samples were analysed by chiral GC for conversion and *ee* determination.

Acknowledgements

We thank the European Commission for financial support (IHP Network grant "Enantioselective Recognition" HPRN-CT-2001-00182). We also like to thank "Merck Research Laboratories" (Merck's Academic Development Program Award to C. Gennari) and Università degli Studi di Milano for financial support and for a postdoctoral fellowship to C. Monti (Assegno di ricerca). U. Piarulli thanks the Dipartimento di Chimica Organica e Industriale (University of Milano) for the hospitality.

[1] For a comprehensive review, see: J. M. Brown, In *Comprehensive Asymmetric Catalysis, Vol. 1* (Eds.: E. N. Jacobsen, A. Pfaltz, H. Yamamoto), Springer, Berlin, **1999**, Chapter 5.1.

[2] For recent reviews, see: a) W. Tang, X. Zhang, *Chem. Rev.* **2003**, *103*, 3029–3069; b) I. D. Gridnev, T. Imamoto, *Acc. Chem. Res.* **2004**, *37*, 633–644.

[3] For a recent review, see: T. Jerphagnon, J.-L. Renaud, C. Bruneau, *Tetrahedron: Asymmetry* **2004**, *15*, 2101–2111; see also: D. Peña, A. J. Minnaard, A. H. M. de Vries, J. G. de Vries, B. L. Feringa, *Org. Lett.* **2003**, *5*, 475–478, and references therein.

[4] For selected references, see: a) M. T. Reetz, G. Mehler, *Angew. Chem.* **2000**, *112*, 4047–4049; *Angew. Chem. Int. Ed.* **2000**, *39*, 3889–3890; b) C. Claver, E. Fernandez, A. Gillon, K. Heslop, D. J. Hyett, A. Martorell, A. G. Orpen, P. G. Pringle, *Chem. Commun.* **2000**, 961–962; c) M. T. Reetz, T. Sell, *Tetrahedron Lett.* **2000**, *41*, 6333–6336; d) D. Peña, A. J. Minnaard, J. G. de Vries, B. L. Feringa, *J. Am. Chem. Soc.* **2002**, *124*, 14552–14553; e) M. van den Berg, A. J. Minnaard, R. M. Haak, R. Leeman, E. P. Schudde, A. Meetsma, B. L. Feringa, A. H. M. de Vries, C. E. P. Maljaars, C. E. Willians, D. Hyett, J. A. F. Boogers, H. J. W. Henderickx, J. G. de Vries, *Adv. Synth. Catal.* **2003**, *345*, 308–323; f) R. Hoen, M. van den Berg, H. Bernsmann, A. J. Minnaard, J. G. de Vries, B. L. Feringa, *Org. Lett.* **2004**, *6*, 1433–1436; g) A. Korostylev, A. Monsees, C. Fischer, A. Borner, *Tetrahedron: Asymmetry* **2004**, *15*, 1001–1005; h) C. W. Lin, C. Lin, L. F.-L. Lam, T. T.-L. Au-Yeung, A. S. C. Chan, *Tetrahedron Lett.* **2004**, *45*, 7379–7381; i) K. Junge, B. Hagemann, S. Enthaler, G. Oehme, M. Michalik, A. Monsees, T. Riermeier, U. Dingerdissen, M. Beller, *Angew. Chem.* **2004**, *116*, 5176–5179; *Angew. Chem. Int. Ed.* **2004**, *43*, 5066–5069; j) K. Junge, B. Hagemann, S. Enthaler, A. Spannenberg, M. Michalik, G. Oehme, A. Monsees, T. Riermeier, M. Beller, *Tetrahedron: Asymmetry* **2004**, *15*, 2621–2631; k) T. Jerphagnon, J.-L. Renaud, P. Demonchaux, A. Ferreira, C. Bruneau, *Adv. Synth. Catal.* **2004**, *346*, 33–36, and references therein; l) M. T. Reetz, J. Ma, R. Goddard, *Angew. Chem.* **2005**, *117*, 416–419; *Angew. Chem. Int. Ed.* **2005**, *44*, 412–415; m) H. Bernsmann, M. van den Berg, R. Hoen, A. J. Minnaard, G. Mehler, M. T. Reetz, J. G. de Vries, B. L. Feringa, *J. Org. Chem.* **2005**, *70*, 943–951, and references therein; n) H. Huang, X. Liu, S. Chen, H. Chen, Z. Zheng, *Tetrahedron: Asymmetry* **2005**, *16*, 693–697, and references therein.

[5] a) M. T. Reetz, T. Sell, A. Meiswinkel, G. Mehler, patent application DE-A 10247633.0 (11-10-2002); b) M. T. Reetz, T. Sell, A. Meiswinkel, G. Mehler, *Angew. Chem.* **2003**, *115*, 814–817; *Angew. Chem. Int. Ed.* **2003**, *42*, 790–793; c) M. T. Reetz, G. Mehler, *Tetrahedron Lett.* **2003**, *44*, 4593–4596; d) M. T. Reetz, G. Mehler, A. Meiswinkel, *Tetrahedron: Asymmetry* **2004**, *15*, 2165–2167; e) M. T. Reetz, X. Li, *Tetrahedron* **2004**, *60*, 9709–9714; f) M. T. Reetz, X. Li, *Angew. Chem.* **2005**, *117*, 3019–3021; *Angew. Chem. Int. Ed.* **2005**, *44*, 2959–2962; g) M. T. Reetz, X. Li, *Angew. Chem.* **2005**, *117*, 3022–3024; *Angew. Chem. Int. Ed.* **2005**, *44*, 2962–2964.

[6] a) D. Peña, A. J. Minnaard, J. A. F. Boogers, A. H. M. de Vries, J. G. de Vries, B. L. Feringa, *Org. Biomol. Chem.* **2003**, *1*, 1087–1089; b) A. Duursma, D. Peña, A. J. Minnaard, B. L. Feringa, *Tetrahedron: Asymmetry* **2005**, *16*, 1901–1904.

[7] See also: a) Y. Yuan, X. Zhang, K. Ding, *Angew. Chem.* **2003**, *115*, 5636–5638; *Angew. Chem. Int. Ed.* **2003**, *42*, 5478–5480; b) K. Ding, H. Du, Y. Yuan, J. Long, *Chem. Eur. J.* **2004**, *10*, 2872–2884, and references therein.

[8] The hetero-complex: homo-complex ratios usually exceed the statistical value, see: A. Duursma, R. Hoen, J. Schuppan, R. Hulst, A. J. Minnaard, B. L. Feringa, *Org. Lett.* **2003**, *5*, 3111–3113.

[9] R. Hoen, J. A. F. Boogers, H. Bernsmann, A. J. Minnaard, A. Meetsma, T. D. Tiemersma-Wegman, A. H. M. de Vries, J. G. de Vries, B. L. Feringa, *Angew. Chem.* **2005**, *117*, 4281–4284; *Angew. Chem. Int. Ed.* **2005**, *44*, 4209–4212.

[10] A. H. M. de Vries, L. Lefort, J. A. F. Boogers, J. G. de Vries, D. J. Ager, *Chimica Oggi* **2005**, March issue.

[11] For recent reviews on combinatorial ligand libraries and high-throughput experimentation in homogeneous catalysis, see: a) C. Gennari, U. Piarulli, *Chem. Rev.* **2003**, *103*, 3071–3100; b) J. G. de Vries, A. H. M. de Vries, *Eur. J. Org. Chem.* **2003**, 799–811.

[12] For an account on atropos/tropos ligands, see: K. Mikami, K. Aikawa, Y. Yusa, J. J. Jodry, M. Yamanaka, *Synlett* **2002**, 1561–1578; for other recent work in this area, see also: a) K. Mikami, S. Kataoka, Y. Yusa, K. Aikawa, *Org. Lett.* **2004**, *6*, 3699–3701; b) P. Scafato, G. Cunsolo, S. Labano, C. Rosini, *Tetrahedron* **2004**, *60*, 8801–8806; c) X. Luo, Y. Hu, X. Hu, *Tetrahedron: Asymmetry* **2005**, *16*, 1227–1231.

[13] Preliminary results of this work were recently communicated, see: C. Monti, C. Gennari, U. Piarulli, *Tetrahedron Lett.* **2004**, *45*, 6859–6862.

[14] a) A. Alexakis, S. Rosset, J. Allamand, S. March, F. Guillen, C. Benhaim, *Synlett* **2001**, *9*, 1375–1378; b) A. Alexakis, C. Benhaim, S. Rosset, M. Humam, *J. Am. Chem. Soc.* **2002**, *124*, 5262–5263; c) A. Alexakis, D. Polet, C. Benhaim, S. Rosset, *Tetrahedron: Asymmetry* **2004**, *15*, 2199–2203; d) A. Alexakis, D. Polet, S. Rosset, S. March, *J. Org. Chem.* **2004**, *69*, 5660–5667.

[15] M. Dieguez, A. Ruiz, C. Claver, *Tetrahedron: Asymmetry* **2001**, *12*, 2895–2900.

[16] a) D. Polet, A. Alexakis, *Tetrahedron Lett.* **2005**, *46*, 1529–1532; b) M. d'Augustin, L. Palais, A. Alexakis, *Angew. Chem.* **2005**, *117*, 1400–1402; *Angew. Chem. Int. Ed.* **2005**, *44*, 1376–1378.

[17] M. T. Reetz, V. Neugebauer, *Angew. Chem.* **1999**, *111*, 134–137; *Angew. Chem. Int. Ed.* **1999**, *38*, 179–181.

[18] G. J. H. Buisman, L. A. van der Veen, A. Klootwijk, W. G. J. de-Lange, P. C. J. Kamer, P. W. N. M. van Leeuwen, D. Vogt, *Organometallics* **1997**, *16*, 2929–2939, and references therein. For a related work, see also: T. P. Clark, C. R. Landis, S. L. Freed, J. Klosin, K. A. Abboud, *J. Am. Chem. Soc.* **2005**, *127*, 5040–5042, and references therein.

[19] a) A. Alexakis, K. Croset, *Org. Lett.* **2002**, *4*, 4147–4149; b) K. Tissot-Croset, D. Polet, A. Alexakis, *Angew. Chem.* **2004**, *116*, 2480–2482; *Angew. Chem. Int. Ed.* **2004**, *43*, 2426–2428; c) O. Equey, A. Alexakis, *Tetrahedron: Asymmetry* **2004**, *15*, 1531–1536.

[20] a) O. Pamies, M. Dieguez, C. Claver, *J. Am. Chem. Soc.* **2005**, *127*, 3646–3647; b) M. Dieguez, O. Pamies, C. Claver, *J. Org. Chem.* **2005**, *70*, 3363–3368.

[21] H. Horibe, K. Kazuta, M. Kotoku, K. Kondo, H. Okuno, Y. Murakami, T. Aoyama, *Synlett* **2003**, *13*, 2047–2051.

[22] For a different approach to a dynamic ligand library, see: D. Tepfenhart, L. Moisan, P. I. Dalko, J. Cossy, *Tetrahedron Lett.* **2004**, *45*, 1781–1783.

[23] Z. Hua, V. C. Vassar, J. Ojima, *Org. Lett.* **2003**, *5*, 3831–3834.

[24] a) A. Rimkus, N. Sewald, *Org. Lett.* **2003**, *5*, 79–80; b) A. van Rooy, D. Burgers, P. C. J. Kamer, P. W. N. M. van Leeuwen, *Recl. Trav. Chim. Pays-Bas* **1996**, *115*, 492–498.

[25] This reactor was developed by Premex in cooperation with DSM; see: http://www.premex-reaktor.ch/d/spezialloesungen/produkteneuheiten/

[26] An alternative explanation is the occurrence of mass-transfer limitation, that is, the catalyzed reaction is too fast compared to the rate of hydrogen diffusion from the gas phase into the solution. This physical process then becomes the rate determining step.

[27] M. J. Burk, G. Casy, N. B. Johnson, *J. Org. Chem.* **1998**, *63*, 6084–6085.

[28] The use of chiral monodentate phosphites containing the biphenol unit had recently been described by Xiao and Chen in the rhodium-catalyzed hydrogenation of dimethyl itaconate, with moderate enantiomeric excess (*ee* max. 75% with **9**-P(O)$_2$O at −15°C; *ee* max. 57% with **9**-P(O)$_2$O at 20°C).[29] The use of a limited number of combinations of different phosphites was also surveyed, and the results were shown to be inferior to the corresponding homocombinations.

[29] W. Chen, J. Xiao, *Tetrahedron Lett.* **2001**, *42*, 8737–8740.

[30] The diastereomers caused by the different conformations of the biphenol unit are not considered in this model.

[31] In principle, the *K* value may be determined experimentally by ^{31}P NMR. However, NMR experiments by using [Rh(cod)$_2$BF$_4$] and various phosphite and phosphoramidite ligands (e.g. **4**-P(O)$_2$O and **13**-P(O)$_2$N) were inconclusive.

[32] W. C. Still, M. Kahn, A. Mitra, *J. Org. Chem.* **1978**, *43*, 2923–2925.
[33] A. Suarez, A. Pizzano, I. Fernandez, N. Khiar, *Tetrahedron: Asymmetry* **2001**, *12*, 633–642.
[34] A. Alexakis, S. Gille, F. Prian, S. Rosset, K. Ditrich, *Tetrahedron Lett.* **2004**, *45*, 1449–1451.
[35] D. J. Aldous, W. M. Dutton, P. G. Steel, *Tetrahedron: Asymmetry* **2000**, *11*, 2455–2462.
[36] D. H. R. Barton, S. Choi, B. Hu, J. A. Smith, *Tetrahedron* **1998**, *54*, 3367–3378.

Received: April 25, 2005
Published online: August 30, 2005

